USGS
science for a changing world

Prepared in cooperation with the
Naval Air Station Patuxent River

Simulation of Ground-Water Flow and Optimization of Withdrawals from Aquifers Underlying the Naval Air Station Patuxent River, St. Mary's County, Maryland

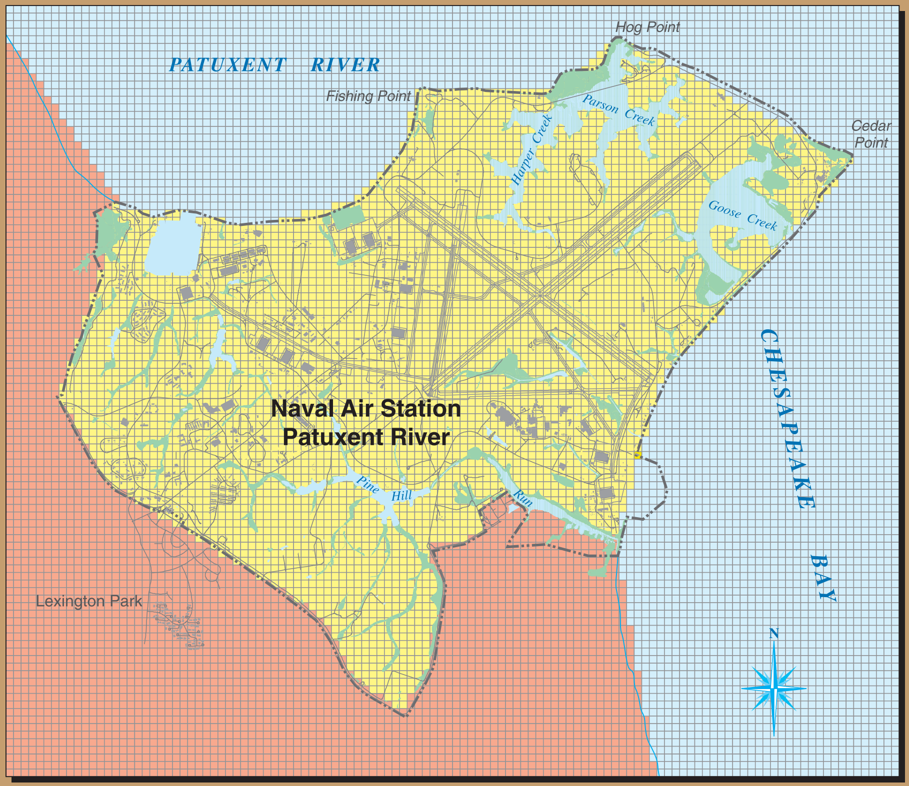

Scientific Investigations Report 2008–5144

U.S. Department of the Interior
U.S. Geological Survey

Cover. Location and design of model grid and water budget zones at Naval Air Station Patuxent River, Maryland.

Simulation of Ground-Water Flow and Optimization of Withdrawals from Aquifers at the Naval Air Station Patuxent River, St. Mary's County, Maryland

By Cheryl A. Dieter and William B. Fleck

Prepared in cooperation with Naval Air Station Patuxent River

Scientific Investigations Report 2008–5144

U.S. Department of the Interior
U.S. Geological Survey

U.S. Department of the Interior
DIRK KEMPTHORNE, Secretary

U.S. Geological Survey
Mark D. Myers, Director

U.S. Geological Survey, Reston, Virginia: 2008

For product and ordering information:
World Wide Web: http://www.usgs.gov/pubprod
Telephone: 1-888-ASK-USGS

For more information on the USGS—the Federal source for science about the Earth, its natural and living resources, natural hazards, and the environment:
World Wide Web: http://www.usgs.gov
Telephone: 1-888-ASK-USGS

Suggested citation:
Dieter, C.A., and Fleck, W.B., 2008, Simulation of ground-water flow and optimization of withdrawals from aquifers at the Naval Air Station Patuxent River, St. Mary’s County, Maryland: U.S. Geological Survey Scientific Investigations Report 2008–5144, 36 p.

Contents

Abstract 1
Introduction....................1
Background....................1
Purpose and Scope 5
Description of Study Area 5
Previous Investigations....................5
Hydrogeologic Framework and Hydraulic Properties of Units 6
Surficial Aquifer 6
Upper Confining Unit 6
Piney Point-Nanjemoy Aquifer 6
Middle Confining Unit....................8
Aquia Aquifer....................8
Lower Confining Unit....................8
Upper Patapsco Aquifer 9
Ground-Water-Flow Model 9
Conceptual Model....................9
Design 10
Model Grid....................10
Boundary Conditions....................12
Model Hydraulic Properties....................13
Model Calibration....................17
Model Sensitivity....................17
Model Limitations....................19
Water Budget 21
Optimization Model....................23
Response Function 23
Application....................23
Scenario 1: Minimize Drawdown of Local Heads 23
Scenario 2: Locate a Second Well for the Northeast Area in the Aquia Aquifer....................24
Suggestions for Future Water-Supply Assessment....................29
Summary and Conclusions....................29
Acknowledgments....................29
Selected References....................30
Glossary....................35
Appendix 1. Specific Capacity Analysis....................36

Figures

1. Map showing location of Naval Air Station Patuxent River, Maryland 2
2. Hydrographs for wells screened in the Piney Point-Nanjemoy, Aquia, and Upper Patapsco aquifers 3
3. Maps showing potentiometric surfaces of the (A) Aquia and (B) Upper Patapsco aquifers in part of southern Maryland, September 2002 4
4. Diagram of the model layering scheme and boundary conditions for the Naval Air Station Patuxent River ground-water-flow model 10
5. Map showing location and design of model grid and water budget zones 11
6. Diagram of model layering, vertical discretization, and boundary conditions along row 60 12
7. Map showing location of observation wells and withdrawal wells simulated in the transient ground-water-flow model at Naval Air Station Patuxent River, Maryland 14
8. Observed and model-simulated hydrographs for well SM Dg 21 screened in the Piney Point-Nanjemoy aquifer from the transient simulation 17
9. Observed and model-simulated hydrographs for six wells screened in the Aquia aquifer from the transient simulation 18
10. Observed and model-simulated hydrographs for two wells screened in the Upper Patapsco aquifer from the transient simulation 19
11. Graph showing results of the steady-state ground-water-flow model sensitivity analysis showing root-mean-squared-error (RMSE) values for the sensitivity-analysis simulations 20
12. Diagram showing simulated net inflows and outflows, in cubic feet per day, for the parts of the Piney Point-Nanjemoy, Aquia, and Upper Patapsco aquifers that underlie the Naval Air Station Patuxent River 22

13–15. Maps showing—
   13. Groupings of wells (A, B, and C) screened in the Aquia aquifer and control node for hypothetical optimization scenario 1 at the Naval Air Station Patuxent River, Maryland 25
   14. Optimal solution for hypothetical optimization scenario 1 at Naval Air Station Patuxent River, Maryland 27
   15. Location of ten potential well sites, including the optimal well site, for hypothetical optimization scenario 2 at Naval Air Station Patuxent River, Maryland 28

Tables

1. Geologic units, corresponding hydrogeologic units, and model layers at Naval Air Station Patuxent River, Maryland 7
2. Ground-water-flow model input values 13
3. Values used to calculate general-head boundary conductance values, and resulting general-head boundary conductance values 13
4. Transient model stress periods with respective time periods and simulated withdrawal rates for the Piney Point-Nanjemoy aquifer, Aquia aquifer, and the stress period total, 1900–2002 15
5. Root-mean-squared-error (RMSE) values for the transient ground-water-flow model simulation 17
6. Water budget for the entire model domain from stress period 106 (December 2002) of the transient model 21
7. Hypothetical scenario 1: optimization model managed wells, steady-state ground-water-flow model withdrawal rates, and optimal withdrawal rates from the optimization model 26
8. Hypothetical scenario 1: optimization model unmanaged wells, steady-state ground-water-flow model withdrawal rates, and withdrawal rates for the optimization model 26

Conversion Factors and Datums

Multiply	By	To obtain
	Length	
inch (in.)	2.54	centimeter (cm)
inch (in.)	25.4	millimeter (mm)
foot (ft)	0.3048	meter (m)
mile (mi)	1.609	kilometer (km)
	Area	
acre	4,047	square meter (m^2)
acre	0.4047	hectare (ha)
acre	0.4047	square hectometer (hm^2)
acre	0.004047	square kilometer (km^2)
square mile (mi^2)	259.0	hectare (ha)
square mile (mi^2)	2.590	square kilometer (km^2)
	Flow rate	
cubic foot per day (ft^3/d)	0.02832	cubic meter per day (m^3/d)
gallon per day (gal/d)	0.003785	cubic meter per day (m^3/d)
	Radioactivity	
picocurie per liter (pCi/L)	0.037	becquerel per liter (Bq/L)
	Specific capacity	
gallon per minute per foot [(gal/min)/ft)]	0.2070	liter per second per meter [(L/s)/m]
	Hydraulic conductivity	
foot per day (ft/d)	0.3048	meter per day (m/d)
	Hydraulic gradient	
foot per mile (ft/mi)	0.1894	meter per kilometer (m/km)
	Transmissivity*	
foot squared per day (ft^2/d)	0.09290	meter squared per day (m^2/d)
	Leakance	
foot per day per foot [(ft/d)/ft]	1	meter per day per meter [(m/d)/m]
inch per year per foot [(in/yr)/ft]	83.33	millimeter per year per meter [(mm/yr)/m]

Temperature in degrees Celsius (°C) may be converted to degrees Fahrenheit (°F) as follows:

°F=(1.8×°C)+32

Vertical coordinate information is referenced to the North American Vertical Datum of 1988 (NAVD 88).

Horizontal coordinate information is referenced to the North American Datum of 1983 (NAD 83).

Altitude, as used in this report, refers to distance above the vertical datum.

*Transmissivity: The standard unit for transmissivity is cubic foot per day per square foot times foot of aquifer thickness [(ft^3/d)/ft^2]ft. In this report, the mathematically reduced form, foot squared per day (ft^2/d), is used for convenience.

Specific conductance is given in microsiemens per centimeter at 25 degrees Celsius (µS/cm at 25 °C).

Concentrations of chemical constituents in water are given either in milligrams per liter (mg/L) or micrograms per liter (µg/L).

Simulation of Ground-Water Flow and Optimization of Withdrawals from Aquifers at the Naval Air Station Patuxent River, St. Mary's County, Maryland

By Cheryl A. Dieter and William B. Fleck

Abstract

Potentiometric surfaces in the Piney Point-Nanjemoy, Aquia, and Upper Patapsco aquifers have declined from 1950 through 2000 throughout southern Maryland. In the vicinity of Lexington Park, Maryland, the potentiometric surface in the Aquia aquifer in 2000 was as much as 170 feet below sea level, approximately 150 feet lower than estimated pre-pumping levels before 1940. At the present rate, the water levels will have declined to the regulatory allowable maximum of 80 percent of available drawdown in the Aquia aquifer by about 2050. The effect of the withdrawals from these aquifers by the Naval Air Station Patuxent River and surrounding users on the declining potentiometric surface has raised concern for future availability of ground water. Growth at Naval Air Station Patuxent River may increase withdrawals, resulting in further drawdown. A ground-water-flow model, combined with optimization modeling, was used to develop withdrawal scenarios that minimize the effects (drawdown) of hypothetical future withdrawals.

A three-dimensional finite-difference ground-water-flow model was developed to simulate the ground-water-flow system in the Piney Point-Nanjemoy, Aquia, and Upper Patapsco aquifers beneath the Naval Air Station Patuxent River. Transient and steady-state conditions were simulated to give water-resource managers additional tools to manage the ground-water resources. The transient simulation, representing 1900 through 2002, showed that the magnitude of withdrawal has increased over that time, causing ground-water flow to change direction in some areas.

The steady-state simulation was linked to an optimization model to determine optimal solutions to hypothetical water-management scenarios. Two optimization scenarios were evaluated. The first scenario was designed to determine the optimal pumping rates for wells screened in the Aquia aquifer within three supply groups to meet a 25-percent increase in withdrawal demands, while minimizing the drawdown at a control location. The resulting optimal solution showed that pumping six wells above the rate required for maintenance produced the least amount of drawdown in the local potentiometric surface.

The second hypothetical scenario was designed to determine the optimal location for an additional well in the Aquia aquifer in the northeastern part of the main air station. The additional well was needed to meet an increase in withdrawal of 43,000 cubic feet per day. The optimization model determined the optimal location for the new well, out of a possible 10 locations, while minimizing drawdown at control nodes located outside the western boundary of the main air station. The optimal location is about 1,500 feet to the east-northeast of the existing well.

Introduction

Beginning in 1998, the U.S. Geological Survey (USGS), in cooperation with Naval Air Station (NAS) Patuxent River, has been investigating the water resources of the Piney Point-Nanjemoy, Aquia, and Upper Patapsco aquifers, which are three principal aquifers extensively used in southern Maryland. The rapid expansion of the NAS Patuxent River in combination with development of the expanding Washington, D.C. suburbs (fig. 1) into Calvert and St. Mary's Counties, has resulted in a population increase in the two counties from 24,000 in 1940 (Forstall, 1995) to 161,000 in 2000 (U.S. Census Bureau, 2003). Water-resource managers, including State, County, and NAS Patuxent River personnel, as well as private citizens, have become deeply concerned with water-supply issues because ground water is the primary source of potable water for most of the two-county region.

Background

NAS Patuxent River started operations in 1942 during World War II as an effort to geographically consolidate Navy and Marine Corps aircraft testing facilities (United States Navy, 2003). NAS Patuxent River has continued to expand since World War II, especially during the early 1950s and the

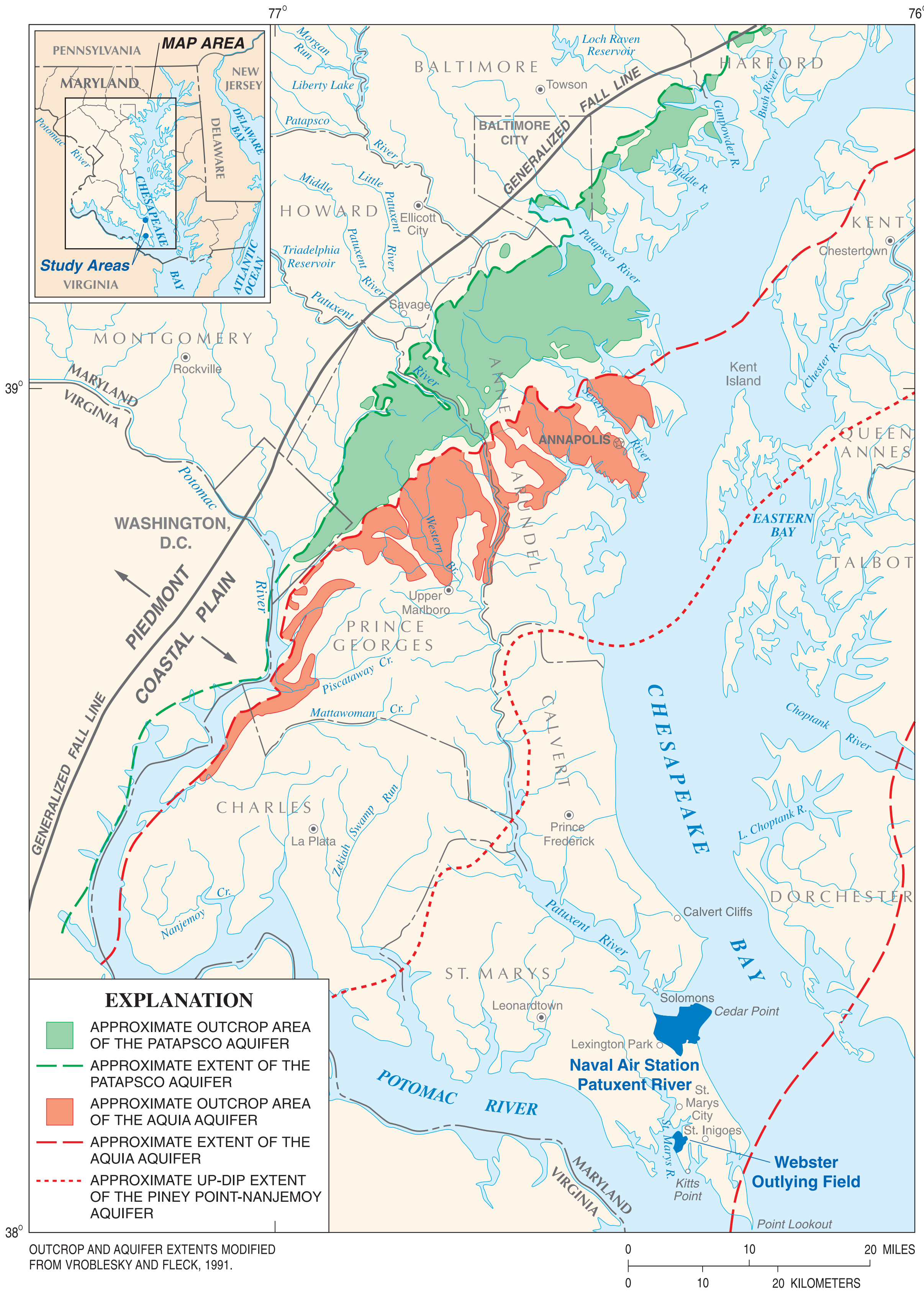

Figure 1. Location of Naval Air Station Patuxent River, Maryland. (From Klohe and Kay, 2007)

1960s. Major reorganizational changes in 1975 resulted in substantial growth both in terms of personnel and in new building construction. On January 1, 1992, the Naval Air Warfare Center Aircraft Division was established and located at NAS Patuxent River. Since the late 1980s, NAS Patuxent River was a receiver base according to the U.S. Department of Defense Base Realignment and Closure (BRAC) Commission, which resulted in a 3.5-percent-per-year increase in the number of employees from 1981 to 1998 (Klohe and Feehley, 2001, p. 2) and a 2.7-percent-per-year increase in the number of employees from 1998 to 2006 (Klohe and Kay, 2007, p. 3).

For the lower part of the southern Maryland region, comprised of Calvert and St. Mary's Counties, a similar population increase of 2.7 percent per year occurred during the 1980s and 1990s. This increase was largely due to the burgeoning of new suburbs outward from the established suburbs of the Annapolis, Maryland, and Washington, D.C. metropolitan centers into the more available and less expensive urban areas of Calvert and St. Mary's Counties. This was also partly a function of the NAS Patuxent River receiver activities, however. The Maryland Department of Planning (2007) projects an increase in population for Calvert and St. Mary's Counties from about 161,000 to 258,000 from 2000 to 2030. With these population projections, there will continue to be ever-increasing pressure on environmental resources, including the ground-water resource. The historical population change and the resulting increase in water use have resulted in well-defined cones of depression in the Aquia and Upper Patapsco aquifers. Water levels in well SM Df 1, which is screened in the Aquia aquifer, were more than 70 ft (feet) below sea level (NAVD 88) by 1984, and continued to drop at about 5 ft/yr (feet per year) through 2002 (fig. 2). The water level in well SM Df 84, which is screened in the Upper Patapsco aquifer, declined from 8 ft below sea level in 1983 to about 48 ft below sea level in 2006, a rate of 1.7 ft/yr (fig. 2). From 1998 through 2006, the water levels in well SM Dg 20, which is screened in the Piney Point-Nanjemoy aquifer, were level at approximately 21 to 25 ft below sea level. The cones of depression in the potentiometric surfaces in the Aquia and Upper Patapsco aquifers as of September 2002 are shown in figure 3.

Ground-water allocations in Maryland are limited by permit to the lowering of potentiometric levels to a maximum of 80 percent of available drawdown. Available drawdown is defined as the total depth from pre-stressed potentiometric levels to the top of the aquifer. The top of the Piney Point-Nanjemoy aquifer is about 200 to 260 ft below sea level, and the top of the Aquia aquifer is about 400 to 500 ft below sea level. Water levels in the Piney Point-Nanjemoy aquifer have recently begun to stabilize in the vicinity of NAS Patuxent River at about 20 to 40 ft below sea level. It is likely that if present (2007) conditions persist, the 80-percent limit is not a concern for the Piney Point-Nanjemoy aquifer. Water levels in the Aquia are much deeper, however, and are presently as much as 170 ft below sea level and falling at rates of about 4 to 5 ft/yr. If the rate of decline of 4 to 5 ft/yr continues, the 80-percent limit would be reached in about 40 to 50 years. Due to the declines in water levels of the Aquia aquifer, there has been an increase in usage of the Upper Patapsco aquifer,

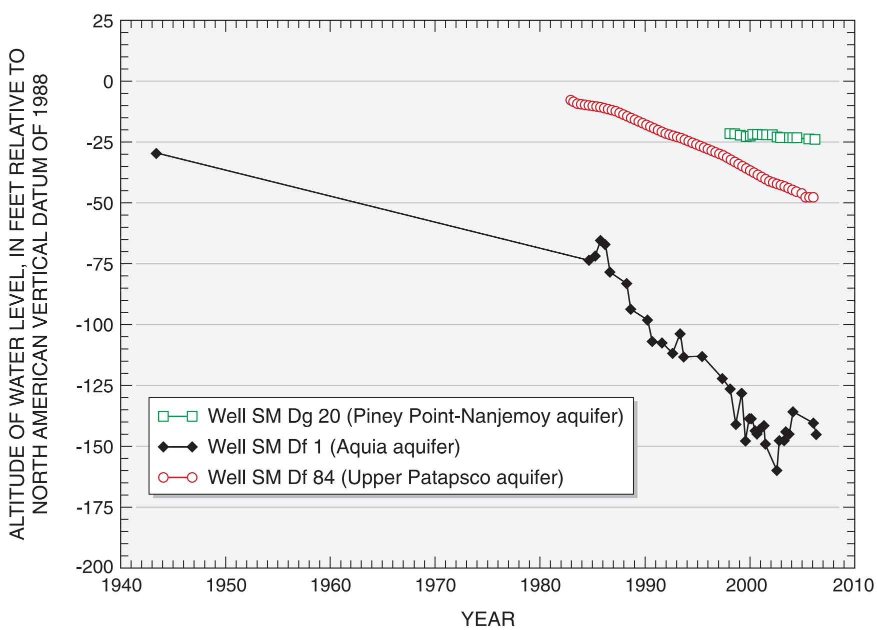

Figure 2. Hydrographs for wells screened in the Piney Point-Nanjemoy, Aquia, and Upper Patapsco aquifers. (Well locations shown in figure 7.)

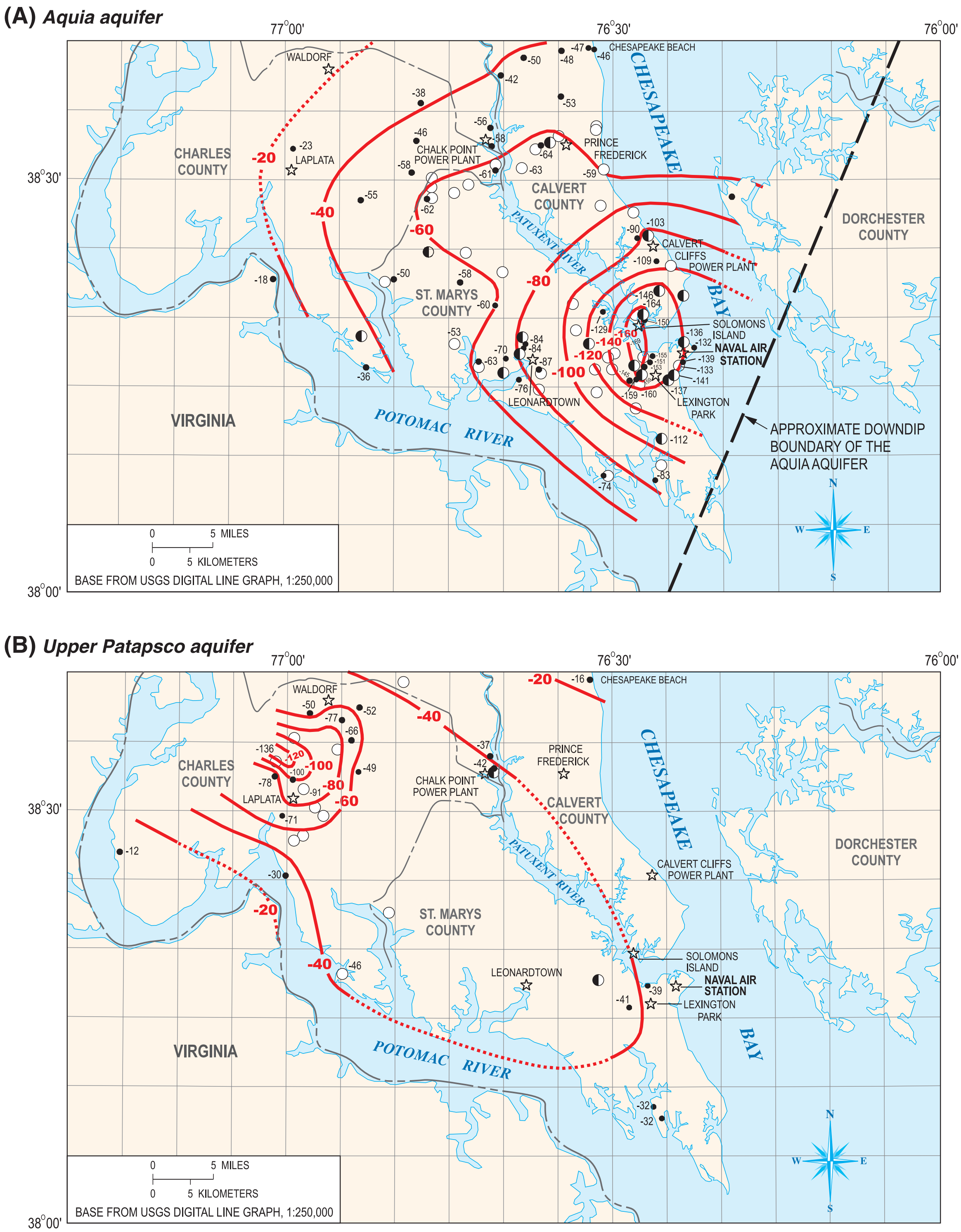

EXPLANATION

-20- - POTENTIOMETRIC CONTOUR – Shows altitude at which water level would have stood in tightly cased wells. Dashed where approximately located. Contour interval 20 feet. National Geodetic Vertical Datum of 1929.

☆ Town or Site Location

WELL – Number is altitude of water level, in feet above or below (-) National Geodetic Vertical Datum of 1929, where water-level measurement is available. Symbol indicates average yield from well or well field, in gallons per day:

- -38 ● Less than 10,000 gallons per day
- -63 ○ 10,000 to 99,999
- -136 ◐ 100,000 to 1,000,000

Figure 3. Potentiometric surfaces of the (A) Aquia and (B) Upper Patapsco aquifers in part of southern Maryland, September 2002. [Modified from Curtin and others (2003a,b)]

where water levels are about 40 to 50 ft below sea level and declining at about 2 to 4 ft/yr. The top of the Upper Patapsco aquifer is more than 600 ft below sea level in this area, however. At the present rate, it would take at least 150 years before the 80-percent limit was reached.

Purpose and Scope

This report describes the development, calibration, and sensitivity analysis of a steady-state and transient ground-water-flow model of the NAS Patuxent River. Applications of an optimization model are presented to demonstrate the potential utility of these models, and the effects of current and future ground-water withdrawals are discussed. Data from published reports, USGS historical well files, the USGS National Water Information System (NWIS), recent water-level measurements, data provided by NAS Patuxent River, and withdrawal data from the USGS State Water-Use Data System (SWUDS) and the Maryland Department of the Environment (MDE) Regulatory Analysis Management System (RAMS) databases were used to create model input files and to calibrate the models.

Description of Study Area

NAS Patuxent River is located in southern Maryland near Lexington Park in St. Mary’s County (fig. 1). NAS Patuxent River encompasses 13,812 acres, including the main air station and Webster Outlying Field (United States Navy, 2003). With a workforce of approximately 20,000 personnel in 2006, NAS Patuxent River was the largest employer in St. Mary’s County. The study area includes the main air station, which is in St. Mary’s County immediately east of Lexington Park and along the right bank of the Patuxent River and the west shore of the Chesapeake Bay (fig. 1).

Previous Investigations

The geology and the hydrogeology of southern Maryland, which includes St. Mary’s and Calvert Counties, have been thoroughly discussed in a number of reports published by both the Maryland Geological Survey (MGS) and the USGS. These reports provide the basic knowledge and data necessary to analyze the interrelation between the geohydrologic framework and natural and manmade transient stresses. An early report by Clark and others (1918, p. 398–411) described both the geology and the water resources of Calvert and St. Mary’s Counties. The water resources of Calvert and St. Mary’s Counties are further described in three MGS Bulletins (Overbeck, 1951; Ferguson, 1953; Otton, 1955). More recently, several publications in the 1970s dealt with either the geology or the water resources of southern Maryland. Brown and others (1972) discussed a large-scale framework of the Coastal Plain sediments. Hansen (1974) discussed various facies trends in the Aquia aquifer within southern Maryland. Weigle and Webb (1970) presented a series of maps describing the water resources of southern Maryland. Hansen and Wilson (1984) reported the results of a deep test well in Lexington Park that was drilled to investigate the potential of aquifers underlying the Aquia aquifer. Klohe and Feehley (2001) published a study of the hydrogeology of the Aquia and Piney Point-Nanjemoy aquifer system that underlies NAS Patuxent River. Klohe and Kay (2007) described the hydrogeology of the Upper Patapsco aquifer that underlies the NAS Patuxent River, and provided ground-water withdrawals and water levels for the Piney Point-Nanjemoy, Aquia, and Upper Patapsco aquifers from the 1940s through April 2006.

Several important publications present information on the location and characteristics of wells and water levels measured in these wells. Drummond (1984) published a compilation of well data for Calvert and St. Mary’s Counties. The USGS compiled water-level-data hydrographs for over 450 wells in southern Maryland for 1946–94 (Curtin and Dine, 1995). Achmad and Hansen (2001a) published a similar report for data from 1970 through 1996.

A series of potentiometric-surface and potentiometric-surface difference maps for the Piney Point-Nanjemoy, Aquia, and Upper Patapsco aquifers have been published. The potentiometric surface is the elevation to which water will rise in tightly cased wells (Fetter, 1994). The difference maps represent changes in the potentiometric surface over some period of years. Achmad and Hansen (2001a, p. 92–93) presented several potentiometric-surface maps for the Piney Point-Nanjemoy aquifer in southern Maryland. A potentiometric-surface map for the Aquia aquifer for spring 1980 (Chapelle and others, 1981) has been followed by a series of potentiometric-surface maps of the Aquia aquifer for almost every year since 1982 and up to the present (Mack and others, 1983a, 1985a, 1987, 1987a, 1989, 1991, 1992b; Curtin and others, 1993a, 1994a, 1995a, 1996a, 1997a, 1999a, 2000a, 2001a, 2002a, 2002c, 2003a, 2005a). Potentiometric-surface-difference maps published for the Aquia aquifer (Mack and others, 1983b, 1985b, 1987b, 1990b, 1992a; Curtin and others, 1994b, 1996b, 1999c, 2001b, 2002e, 2005b) show changes in the potentiometric surface for periods as short as 1 year to as long as 19 years. Part of the potentiometric surface of the Aquia aquifer for 2002 is shown in figure 3a (Curtin and others, 2003a). Mack and others (1992c) published a potentiometric-surface map for the Upper Patapsco aquifer for 1990. Curtin and others (1993b, 1994c, 1995b, 1996c, 1997b, 1999b, 2000b, 2001c, 2002b, 2002d, 2003b, 2005c) continued to publish potentiometric-surface maps for the Upper Patapsco aquifer for essentially every year from 1991 to 2005. Achmad and Hansen (2001a, p. 94) presented a potentiometric-surface-difference map for 1980–1996 for the Upper Patapsco aquifer. Curtin and others (1999d, 2001d, 2002f, 2005d) published potentiometric-surface-difference maps for the Upper Patapsco aquifer that compare 1990 to 1997, 1999, 2001, and 2003. Part of the potentiometric surface of the Upper Patapsco aquifer for 2002 is shown in figure 3b (Curtin and others, 2003b).

A number of reports that describe the results of digital ground-water-flow models that include NAS Patuxent River are available. Kapple and Hansen (1976) reported on the results of a ground-water-flow model of the Aquia aquifer in southern Maryland that was centered at NAS Patuxent River. The results of two large-scale models that included the complete wedge of Coastal Plain sediments of Maryland and Delaware (Fleck, 1983; Fleck and Vroblesky, 1996) describe the generalized flow system for the complete set of aquifers at NAS Patuxent River. A more refined model of the Aquia and Piney Point-Nanjemoy aquifers underlying southern Maryland was completed by Chapelle and Drummond (1983). More recently, reports on the results and application of a ground-water model that simulates flow conditions within the Aquia and Piney Point-Nanjemoy aquifers underlying Calvert and St. Mary's Counties have been published (Achmad and Hansen, 1997, 2001a, 2001b, and Achmad and Fewster, 2003). In addition, Drummond (2005) developed a ground-water-flow model to simulate the water-supply potential of the Coastal Plain aquifers including the Piney Point-Nanjemoy, Aquia, Upper Patapsco, and Lower Patapsco aquifers in Calvert, Charles, and St. Mary's Counties, Maryland. All of these models provided important results for the purposes for which they were designed; however, additional modeling was needed to refine the grid, to more accurately define the individual wells at the main air station, and to allow for optimization of withdrawals from wells.

Hydrogeologic Framework and Hydraulic Properties of Units

The geologic formations underlying NAS Patuxent River are part of the Coastal Plain Physiographic Province. These unconsolidated sediments are composed of beds of clays, silts, sands, and gravels. The thickness of the Coastal Plain sediments is approximately 2,600 ft in the vicinity of NAS Patuxent River (Hansen and Wilson, 1984), and they range in age from Early Cretaceous to Quaternary (Achmad and Hansen, 1997, p. 6) (table 1). The bedding strike of the Coastal Plain sediments in the vicinity of NAS Patuxent River is north-northeast, and the dip is to the east-southeast at an angle of approximately 0.1 to 0.3 degrees (Vroblesky and Fleck, 1991, p. 12, 15, 29, 31). Underlying the unconsolidated Coastal Plain sediments are mostly indurated metamorphic rocks of Paleozoic age (Achmad and Hansen, 1997, p. 6). The hydrogeologic units discussed in this report from youngest to oldest are: the surficial aquifer, the upper confining unit, the Piney Point-Nanjemoy aquifer, the middle confining unit, the Aquia aquifer, the lower confining unit, and the Upper Patapsco aquifer (table 1; fig. 4). Although there are Cretaceous units between the Patapsco aquifer and the Paleozoic rocks, they are not discussed in this report because they are below the section of interest.

Surficial Aquifer

The surficial aquifer in the vicinity of the NAS Patuxent River is composed of mostly undifferentiated sediments ranging in grain size from clay to gravel. These sediments underlie most of the main air station and range in age from early Pleistocene to Holocene and consist of sand, gravel, silt, and clay of the early Pleistocene Chicamuxen Church Formation; the late Pleistocene Omar, Maryland Point, and Kent Island Formations; and undifferentiated Holocene deposits. The oldest sediments of the surficial aquifer are the upland deposits on the west side of the main air station. These consist of sands and gravels of the late Pliocene age Park Hall Formation and Upland gravel (McCartan, 1989). The hydraulic properties of the surficial aquifer have not been tested within the study area.

Upper Confining Unit

The upper confining unit consists of three Miocene formations deposited under marine conditions, which in decreasing age are the Calvert, Choptank, and St. Mary's Formations (Achmad and Hansen, 1997, p. 8). These three formations form the Chesapeake Group in southern Maryland. The Calvert Formation, which is about 150 ft thick, consists principally of olive gray to olive brown silt and clay, and some fine sand. The 10- to 20-ft basal part, which consists of sand and some gravel, is effectively a part of the underlying Piney Point-Nanjemoy aquifer. The Choptank Formation, which overlies the Calvert Formation, is principally composed of grayish-green silty clays interbedded with some highly fossiliferous fine sand, and ranges from 30 to 100 ft thick. The thinner St. Mary's Formation, which is generally less than 50 ft in thickness, overlies the Choptank Formation. This formation is more blue in color than the underlying Choptank Formation, but is otherwise a very similar deposit of interbedded silty clay and fine sand.

Chapelle and Drummond (1983, table 2) reported six vertical hydraulic conductivity values for the clayey part of the Chesapeake Group. These values were calculated by laboratory methods and range from 6×10^{-5} to 2×10^{-2} ft/d. This range of values is consistent with values for marine clays as reported in standard texts (Domenico and Schwartz, 1990, table 3.2; Freeze and Cherry, 1979, table 2.2; Fetter, 1994, table 4.6).

Piney Point-Nanjemoy Aquifer

Underlying the Chesapeake Group marine clays are a sequence of sandy deposits that structurally form the Piney Point-Nanjemoy aquifer (table 1). The geologic formations include the upper part of the lower Eocene Nanjemoy Formation, the middle Eocene Piney Point Formation, an unnamed Oligocene(?) bed that may correlate with the Old Church Formation (Achmad and Hansen, 1997, p. 12), and the lower

Table 1. Geologic units, corresponding hydrogeologic units, and model layers at Naval Air Station Patuxent River, Maryland. [Modified from Klohe and Kay, 2007]

<table>
<tr><th>System</th><th>Series</th><th colspan="2">Group or Geologic Unit</th><th>Hydrogeolgic Unit,
(Model Layer Number)</th></tr>
<tr><td>Quaternary</td><td>Holocene to Pleistocene</td><td colspan="2" rowspan="2">Surficial units (undifferentiated)</td><td rowspan="2">Surficial aquifer
(Layer 1)</td></tr>
<tr><td rowspan="11">Tertiary</td><td>Pliocene</td></tr>
<tr><td rowspan="3">Miocene</td><td rowspan="3">Chesapeake Group
(undivided)</td><td>St. Mary's Formation</td><td rowspan="3">Upper confining unit
(Layer 2)</td></tr>
<tr><td>Choptank Formation</td></tr>
<tr><td>Calvert Formation</td></tr>
<tr><td>Oligocene (?)</td><td colspan="2">unnamed Oligocene (?) Miocene (?) beds</td><td rowspan="3">Piney Point-Nanjemoy aquifer
(Layer 3)</td></tr>
<tr><td rowspan="3">Eocene</td><td colspan="2">Piney Point Formation</td></tr>
<tr><td colspan="2" rowspan="2">Nanjemoy Formation</td></tr>
<tr><td rowspan="2">Middle confining unit
(Layer 4)</td></tr>
<tr><td rowspan="3">Paleocene</td><td colspan="2">Marlboro Clay</td></tr>
<tr><td colspan="2">Aquia Formation</td><td>Aquia aquifer
(Layer 5)</td></tr>
<tr><td colspan="2">Brightseat Formation</td><td rowspan="2">Lower confining unit
(Layer 6)</td></tr>
<tr><td rowspan="2">Cretaceous</td><td rowspan="2">Lower Cretaceous</td><td colspan="2" rowspan="2">Patapsco Formation
(of the Potomac Group)</td></tr>
<tr><td>Upper Patapsco aquifer
(Layer 7)</td></tr>
</table>

part of the Miocene Calvert Formation, which is the lower part of the Chesapeake Group (table 1). The total thickness of this aquifer in the vicinity of the NAS Patuxent River is about 45 to 75 ft.

The Nanjemoy Formation is a coarsening-upward sequence from dark greenish-gray sandy clays to olive or olive-brown clayey sands. Glauconite is common to abundant throughout this section. The lower part of this sequence, which is predominantly clay, is the uppermost sequence of the middle confining unit. The formation crops out in a small band principally in eastern Prince George's and southern Anne Arundel Counties. The overlying Piney Point Formation is predominantly composed of glauconitic sand that is gray to grayish-green, medium- to coarse-grained, and well sorted. The Piney Point Formation does not crop out, but rather pinches out across central Calvert and northern St. Mary's Counties. The Oligocene(?) deposit that overlies the Piney Point is thin and discontinuous and is composed of clayey quartz sand (Achmad and Hansen, 1997, p. 12). The thickness of this bed is about 1 to 1.5 ft. As a consequence, it is not possible to distinguish this bed in the subsurface from the overlying Calvert Formation, which is the oldest unit of the Chesapeake Group in the model area, and is about 150 ft thick. The basal 10 to 20 ft of the Calvert Formation consists of fine to medium sand with some gravel that crops out in a narrow belt adjacent to and downdip from the Nanjemoy Formation in Anne Arundel, Prince George's, and Charles Counties (Cooke and Cloos, 1951; Glaser, 1976; Mathews, 1933; Hansen, 1972, p. 79, 115; Hack, 1977; Achmad and Hansen, 1997, p. 10).

The horizontal hydraulic conductivity of both the Nanjemoy and Piney Point Formations is generally in the range of 5 to 20 ft/d. Hansen (1972) reported a value of 16 ft/d for the Piney Point Formation from a test at Lexington Park. In the vicinity of the NAS Patuxent River, the transmissivity is approximately 400 ft^2/d (feet squared per day) and the thickness is about 50 ft (Williams, 1979, plate 5, fig. 5); thus, the horizontal hydraulic conductivity would be about 8 ft/d. The specific capacity of wells in the vicinity of the main air station (Drummond, 1984, table 3) was used to calculate horizontal hydraulic conductivities. The procedure used is described in Appendix 1. For 11 wells screened in the Piney Point-Nanjemoy aquifer, the median value was 15 ft/d (Appendix 1). The mean value of 10 ft/d for horizontal hydraulic conductivity is consistent with a fine- to medium-sorted sand as reported in standard texts (Domenico and Schwartz, 1990, table 3.2; Freeze and Cherry, 1979, table 2.2; Fetter, 1994, table 4.6). Storage coefficient values of 0.0003 to 0.0004 were reported by Hansen (1972), 0.00009 to 0.0004 by Williams (1979), and 0.0004 by Chapelle and Drummond (1983). Williams (1979) used a storage coefficient of 0.0003 for the Piney Point-Nanjemoy aquifer in a ground-water-flow model, and Chapelle and Drummond (1983) used a storage coefficient of 0.0004 for the Piney Point-Nanjemoy aquifer in a ground-water-flow model.

Middle Confining Unit

The middle confining unit directly underlies the Piney Point-Nanjemoy aquifer in the model area. The sediments of this unit are composed of the lower part of the lower Eocene Nanjemoy Formation, and the underlying lower Eocene and upper Paleocene Marlboro Clay (Achmad and Hansen, 1997, p. 17). The total thickness of this unit in the vicinity of the NAS Patuxent River as described by Achmad and Hansen (1997, fig. 6) is about 90 ft; however, Chapelle and Drummond (1983, fig. 6) and Klohe and Feehley (2001, p. 13 and fig. 6) calculated a thickness of about 140 ft. The thickness of the part of the middle confining unit that underlies the NAS Patuxent River for the model described in this report ranges from 123 to 170 ft.

The lower part of the Nanjemoy Formation, which directly underlies the Piney Point-Nanjemoy aquifer, is composed of greenish to black olive-black silts and clays. The bottom section of the middle confining unit, the Marlboro Clay, is composed of pale red or gray plastic clay (Achmad and Hansen, 1997; Klohe and Feehley, 2001). The difference in the composition of the sediments between the upper and lower part of the middle confining unit is reflected in the hydraulic conductivity values at various depths within the unit. Values of hydraulic conductivity from the confining part of the Nanjemoy Formation in Kent Island, Queen Anne's County ranged from 6.6×10^{-3} to 6.9×10^{-2} ft/d (Kapple and Hansen, 1976, table 2). Two values for vertical hydraulic conductivity for the Marlboro Clay from locations within 10 mi (miles) of the NAS Patuxent River were 5.8×10^{-5} and 9.5×10^{-5} ft/d (Chapelle and Drummond, 1983, table 2). These two vertical hydraulic conductivity values for the Marlboro Clay fall within the expected range for marine clay of about 5×10^{-6} to 3×10^{-3} ft/d (Fetter, 1994, p. 98; Freeze and Cherry, 1979, p. 29; Domenico and Schwartz, 1990, p. 65). Due to stratification, it is necessary to use a weighted harmonic mean to calculate an average vertical hydraulic conductivity value for the full thickness of the confining unit (Lee and Fetter, 1994, p. 22). Assuming a thickness of 120 ft and a vertical hydraulic conductivity of 4×10^{-2} ft/d for the Nanjemoy part of the unit and for the Marlboro Clay, values of 30 ft and 8×10^{-5} ft/d, respectively, the weighted harmonic mean for vertical hydraulic conductivity is about 4×10^{-4} ft/d for the full thickness. This value is consistent with a value of 5×10^{-4} ft/d used in the model developed by Achmad for southern Maryland (Achmad and Hansen, 1997, p. 19).

Aquia Aquifer

The Aquia aquifer correlates with the upper Paleocene Aquia Formation (Achmad and Hansen, 1997, p. 19), which underlies the upper Paleocene Marlboro Clay and overlies the lower Paleocene Brightseat Formation. The recharge area for the Aquia aquifer, which is the outcrop belt that extends across central Anne Arundel County and into east-central Prince George's County, is located about 40 to 50 mi to the northwest of the NAS Patuxent River (fig. 1). This recharge area is sub-parallel to and just to the northwest of the recharge area for the Piney Point-Nanjemoy aquifer. A sandy to clayey facies change occurs about 5 mi downdip from NAS Patuxent River (Hansen, 1972, p. 64). The top of the aquifer is at an elevation of about 450 ft below sea level (NAVD 88) and the thickness is about 100 ft (Achmad and Hansen, 1997, p. 22). The sediments of the Aquia aquifer were deposited on a shoaling marine shelf that resulted in a coarsening-upward sequence. The lower quarter of the Aquia aquifer is generally a poorly sorted clayey to fine-grained sand with thin, calcareously cemented sandstone and shell layers. The upper part is a coarser-grained, well-sorted sand, also with thin shelly beds throughout. Green to black, well-sorted, medium to coarse glauconite is abundant throughout the upper three quarters of the Aquia aquifer. This gives it a "salt and pepper" appearance.

Hansen (1972, p. 66) lists three "transmissibility" values ranging from 5×10^3 to 7.5×10^3 gallons per day per foot (670 to 1,000 ft^2/d) for locations within about 10 mi of NAS Patuxent River. Horizontal hydraulic conductivity is calculated by dividing the transmissibility of the aquifer by the thickness of the aquifer. The thickness at these locations ranges from 110 to 150 ft and thus, the horizontal hydraulic conductivity for Hansen's values averaged about 5 ft/d. A median value of 20 ft/d was calculated from 30 specific capacity values as described in Appendix 1. A storage coefficient value determined from a pumping test at Lexington Park, St. Mary's County, was 0.0002 (Hansen, 1972, p. 66). Eight other values from the Aquia aquifer throughout Maryland ranged from 0.0001 to 0.0004, with a median value of 0.0002 (Hansen, 1972, p. 66). Storage coefficient values for the Aquia aquifer used in three previous models were 0.0001 (Achmad and Hansen, 1997, p. 20), 0.0003 (Kapple and Hansen, 1976, p. 20), and 0.0001 (Chapelle and Drummond, 1983, p. 44).

Lower Confining Unit

The lower confining unit consists of sediments of the Paleocene Brightseat Formation and the uppermost sediments of the Patapsco Formation of Early Cretaceous age. The Late Cretaceous formations throughout much of Maryland, which include the Monmouth, Matawan, and Magothy Formations, are missing in the lithologic section in the vicinity of the NAS Patuxent River. The Brightseat Formation is typically gray to grayish black, micaceous clay and silt with some fine sand lenses (Achmad and Hansen, 1997, p. 7). The fine sand layers provide minimal water to a few domestic wells. The Brightseat Formation in the area of the NAS Patuxent River is about 50 ft thick. The lower half of the lower confining unit is composed of the uppermost 50 to 90 ft of the Patapsco Formation. This section of the Patapsco Formation principally consists of a red plastic clay (Vroblesky and Fleck, 1991, p. 16). The total thickness of the lower confining unit is about 110 to 140 ft (Klohe and Kay, 2007).

The hydrologic properties of the lower confining unit have not been extensively measured. An analysis of a Brightseat core from Prince George's County indicated values for hydraulic conductivity and specific storage of 9.5 x 10^{-4} ft/d and 7.4 x 10^{-5} ft^{-1}, respectively (Hansen, 1977, p. 12). Assuming a thickness of about 125 ft in the NAS Patuxent River area, the storage coefficient would be about 0.009. Laboratory analyses of a core from the Patapsco Formation that was 64 percent clay indicated hydraulic conductivity values of 1 x 10^{-5} and 7 x 10^{-6} ft/d (Mack, 1974, p. 16).

Upper Patapsco Aquifer

The Upper Patapsco aquifer, which is Early Cretaceous in age, immediately underlies the lower confining unit in the vicinity of the NAS Patuxent River. The sediments are composed of about 200 ft of medium- to fine-grained sand, some gravel, and interbeds of gray clay (Klohe and Kay, 2007). The top of the aquifer is located at an elevation of about 680 ft below sea level. Recharge to the Upper Patapsco aquifer occurs in the subcrop area, which extends as a narrow band to the east and sub-parallel to the Fall Line, which is the approximate boundary between the Coastal Plain and Piedmont Physiographic Provinces (fig. 1). The upper and lower parts of the Patapsco aquifer are not differentiated in various areas of Maryland, as well as in various reports such as Hansen (1972); therefore, in instances where upper and lower are not specified, the aquifer is referred to as the Patapsco aquifer.

Transmissibility values for the Patapsco aquifer determined from aquifer tests that were reported by Hansen (1972, p. 34) for Charles County ranged from 1,000 to 5,000 gallons per day per foot (135 to 670 ft^2/d). The thickness of the Patapsco ranged from 75 to 105 ft, resulting in a horizontal hydraulic conductivity of 8 to 58 ft/d, with a median value of 13 ft/d. The results of an aquifer pump test at NAS Patuxent River production well SM Df 100 indicated a transmissivity value of about 3,900 ft^2/d (Klohe and Kay, 2007). The well has 60 ft of screen over a thickness of 200 ft (Klohe and Kay, 2007). Thus, the horizontal hydraulic conductivity at this location is about 65 ft/d, which is higher than the value of 45 ft/d obtained from the specific capacity calculations in Appendix 1 for the same well. Analysis of another aquifer test at the NAS Patuxent River Webster Outlying Field for the Upper Patapsco well SM Ff 65 indicated a transmissivity value of 2,100 ft^2/d (Klohe and Kay, 2007). Well SM Ff 65 has 50 ft of screen over a thickness of 239 ft (Klohe and Kay, 2007). Thus, the hydraulic conductivity is on the order of 10 ft/d. Hansen (1972, p. 34) reported values for storage coefficients for the Patapsco aquifer; values in Charles and Prince George's Counties ranged from 0.0001 to 0.0004.

A confining unit, composed of beds of clay with low vertical hydraulic conductivity, lies beneath the Upper Patapsco aquifer. Achmad and Hansen (2001a) referred to the unit as the Patapsco Confining Bed and determined that it is approximately 300 ft thick at Lexington Park.

Ground-Water-Flow Model

The following sections describe the ground-water-flow model designed to simulate the aquifers underlying NAS Patuxent River, including the conceptual model, and the design, input parameters, calibration, and sensitivity of the numerical flow model. Two simulations of the ground-water-flow model are presented in this report: a three-dimensional transient simulation, and a three-dimensional steady-state simulation. The transient and steady-state simulations use the same model grid and input parameters. The purpose of the transient simulation was to calibrate the model to observed (measured) water levels recorded over the past 50 years and to simulate the changes in ground-water head gradients (fluxes and directions) from pre-stressed conditions in the early 1900s to stressed conditions beginning in the 1940s, and continuing through 2002. The steady-state model was constructed in order to link the ground-water-flow model simulating flow conditions at the end of 2002 with an optimization model code.

The USGS MODFLOW-96 code (McDonald and Harbaugh, 1984), updated in 1996 by Harbaugh and McDonald (1996), was used to mathematically simulate ground-water flow and calculate ground-water budgets. The MODFLOW code uses finite-difference techniques to solve the partial differential equations that describe ground-water flow. Processing MODFLOW graphical-user interface (PMWIN) (Chiang and Kinzelbach, 1998) was used as the pre- and post-processing software program, enhancing the capabilities of MODFLOW. PMWIN tools were used to interpret MODFLOW output by extracting, plotting, and calculating water budgets for subsets of the modeled area.

Conceptual Model

The conceptual model is a representation of the current understanding of the components of the ground-water-flow system that underlie NAS Patuxent River. The conceptual model attempts to describe how water enters the system, how it moves through the system, how much is stored in the system, and finally, how it exits the system. Essentially, it is a synthesis of the geologic framework, recharge conditions, hydraulic parameters, and discharge conditions (including withdrawal rates).

The conceptual model, shown in figure 4, encompasses a layered system of aquifers and confining units. These layers, described in the previous section, include (from top to bottom) the surficial aquifer, upper confining unit, Piney Point-Nanjemoy aquifer, middle confining unit, Aquia aquifer, lower confining unit, and the Upper Patapsco aquifer. The topmost layer represents the surficial aquifer. The heads in this layer remain relatively constant and there is minimal interaction with the next lower aquifer. The confining layers restrict flow between aquifers. In the model region, inflows are primarily lateral fluxes from outside the model region. Vertical fluxes occur between layers as a result of hydraulic gradients. Some water is stored in the aquifers and confining units. Outflow from the ground-water-flow system underlying the NAS Patuxent River under pre-stressed conditions was mostly lateral discharge. During stressed conditions, the substantial pumping withdrawals from the aquifers account for much of the discharge out of the system.

Design

The design of the transient and steady-state ground-water-flow simulations includes horizontal and vertical discretization of space representing the aquifer and confining unit layers, boundary conditions, and input parameters such as hydraulic conductivity and pumping withdrawals. The design is the same for both the steady-state and transient simulations with the following exceptions: the transient model simulation includes time discretization, storage coefficients, variable withdrawals, and time-specified boundary heads.

Model Grid

The model encompasses an area of 5.6 by 4.8 mi, approximately 27 mi^2 (square miles). The horizontal extent of the model, in relation to the main air station boundary, and cell discretization are shown in figure 5. The grid is composed of 118 columns and 102 rows. There are a total of 84,252 cells, each 250 ft wide by 250 ft long, with each cell representing an area of 62,500 ft^2 (square feet), or approximately 1.4 acres. The cell size is small to adequately represent variations in hydraulic properties, and to simulate pumping effects. In comparison, the cell sizes for the southern Maryland model by Achmad and Hansen (1997) and the Drummond (2005) model are both approximately 110 times larger than the cell size for the NAS Patuxent River model.

The vertical discretization of the model was designed to encompass the three aquifers from which NAS Patuxent River withdraws water, as well as the intervening confining units, and the shallow surficial aquifer as an upper boundary condition. Thus, the model encompasses seven layers, which are shown in table 1, and are numbered from top to bottom (figs. 4 and 6). Layer thickness and hydraulic properties are presented in table 2. Model layer 1 represents the surficial unconfined aquifer underlying NAS Patuxent River; this aquifer is not tapped for potable water by the main air station, but is included in the model as a model boundary condition. Layer 1, as represented by the model, ranges in thickness from 10 to 101 ft. Achmad and Hansen (1997, fig. 2, p. 9) indicate a possible paleochannel underlying NAS Patuxent River with thicknesses of the surficial aquifer up to 130 ft. For the NAS Patuxent River model, however, the simulated thickness is not critical because layer 1 is (1) simulated as a constant head

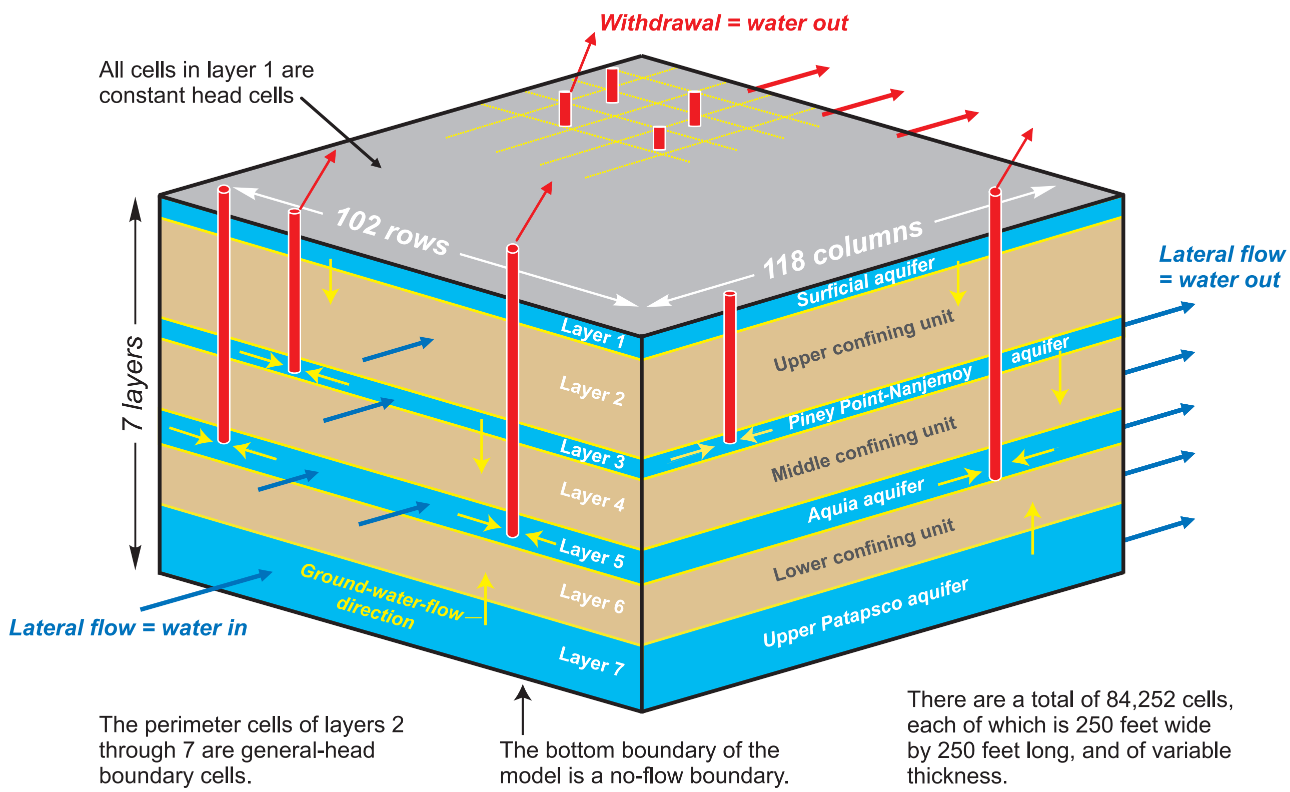

Figure 4. Diagram of the model layering scheme and boundary conditions for the Naval Air Station Patuxent River ground-water-flow model.

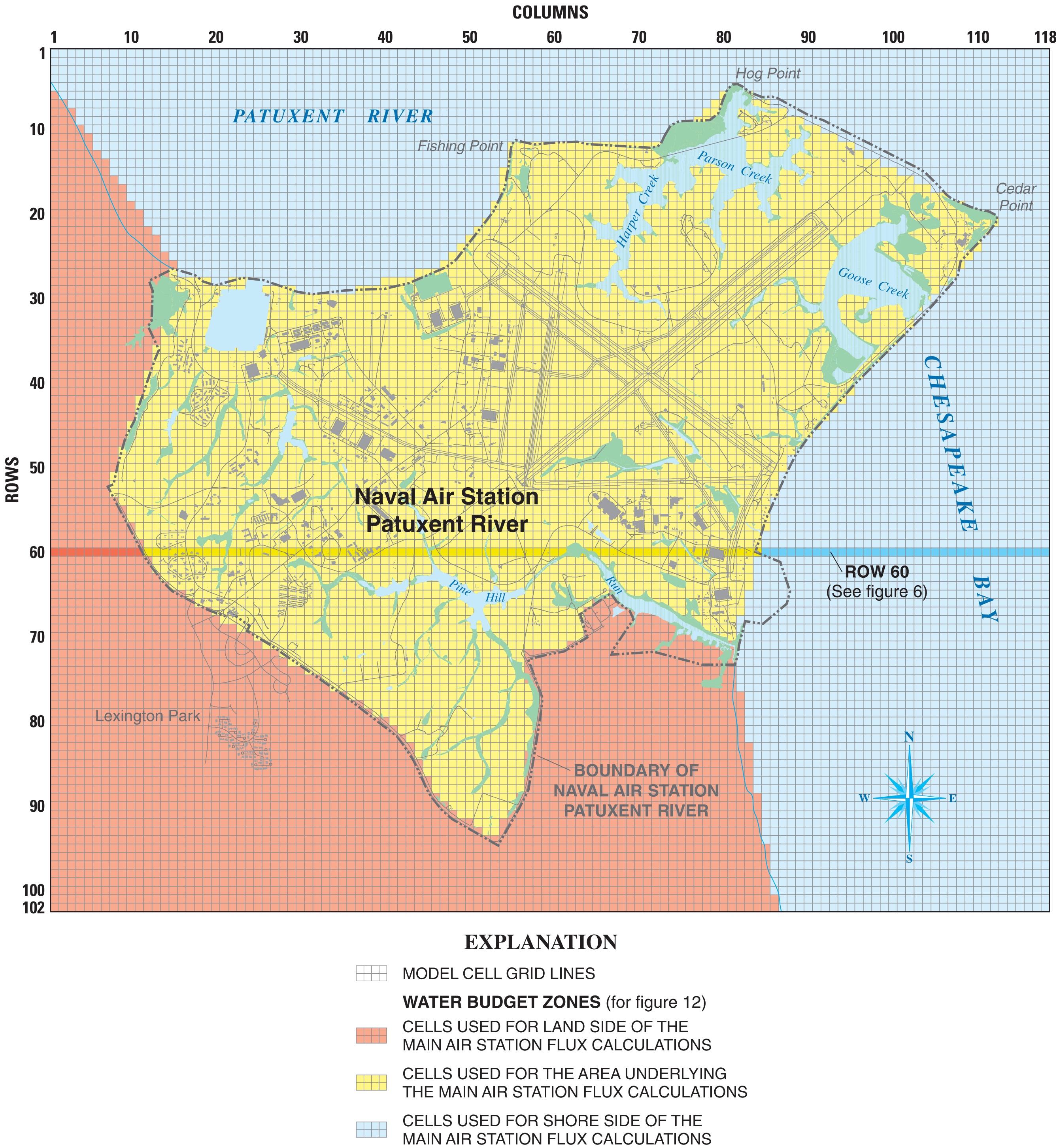

Figure 5. Location and design of model grid and water budget zones.

boundary condition, and (2) underlain by a thick layer of silt and clay (figs. 4 and 6). Layer 2, which represents the upper confining unit, ranges in thickness from 190 to 265 ft. Layer 3 represents the Piney Point-Nanjemoy aquifer. The thickness of the Piney Point-Nanjemoy aquifer underlying NAS Patuxent River ranges from 45 to 75 ft. Layer 4 represents the middle confining unit, and ranges in thickness from 123 to 185 ft. Layer 5 represents the Aquia aquifer, one of the principal aquifers in southern Maryland, and ranges in thickness from 70 to 144 ft. Layer 6 represents the lower confining unit, and ranges in thickness from 45 to 120 ft. The bottom model layer (layer 7) represents the Upper Patapsco aquifer, and is 200 ft in thickness (Klohe and Kay, 2007).

Boundary Conditions

There are three different types of boundary conditions in the model (figs. 4 and 6). The uppermost layer (layer 1) represents the surficial aquifer, and is a constant-head boundary. The constant-head values in this layer ranged from 0.5 to 91 ft above sea level. These values, which are a rough reflection of the topography, were calculated by digitizing the topography and then adjusting for an approximated thickness of the unsaturated zone (or depth to the saturated zone). The constant heads of layer 1 represent an average water level in each model cell. Recharge is not input into the model because layer 1 is represented as a constant-head boundary. The thickness of the upper confining unit, which is represented as model layer 2, ranges from 190 to 265 ft thick, resulting in minimal interaction between layer 1 and the rest of the model. Thus, the representation of the water levels in layer 1 is not critical to the model results and representing this layer as a constant head is justified.

The bottom of layer 7 is represented in the model as a no-flow boundary. The laterally discontinuous nature of the clays, silts, and sands within the Upper Patapsco aquifer makes it difficult to delineate the lower boundary. However, Achmad and Hansen (2001a) describe the Patapsco Confining Bed as approximately 300 ft thick at Lexington Park. Borehole geophysical logs from wells near the air station indicate local layers of low-permeability silts and clays that are able to retard vertical flow. Therefore, the use of a no-flow boundary is justified.

The third boundary condition, a general-head boundary, encompasses the perimeters of layers 2–7. A general-head boundary specifies both a head at some distance from the general-head boundary cell and a conductance of the material between the distant head and the physical model boundary (McDonald and Harbaugh, 1984, p. 347). The general-head boundary was used because no close natural hydrologic boundaries exist. Extending the model domain to the natural boundaries would have likely resulted in larger model grid cells reducing accuracy within the study area, and an expansion of model development beyond the scope of the study.

The specified heads along the boundaries of model layers 3,5, and 7, which represent the Piney Point-Nanjemoy, Aquia, and Upper Patapsco aquifers, respectively, were derived from published potentiometric maps for these aquifers (Achmad and Hansen, 2001a, figs. 14, 15, 85, 86, 92, 93, map nos. S-13 to 18, S-25 to 34; Fleck and Vroblesky, 1996, pl. 2; Achmad and Hansen, 1997, figs. 20-23). The specified heads along the boundaries of model layers 2, 4, and 6, which represent the confining units, were estimated by calculating the mean value between the aquifer heads from the aquifer layers above and below. A linear hydraulic gradient was assumed between aquifers. For the transient model, general-head boundary conditions are specified for each stress period. For some stress periods, published head maps were not available; therefore, heads were interpolated from head maps from the nearest time periods. For the steady-state model, the general-head boundary conditions specified for the December 2002 stress period were used.

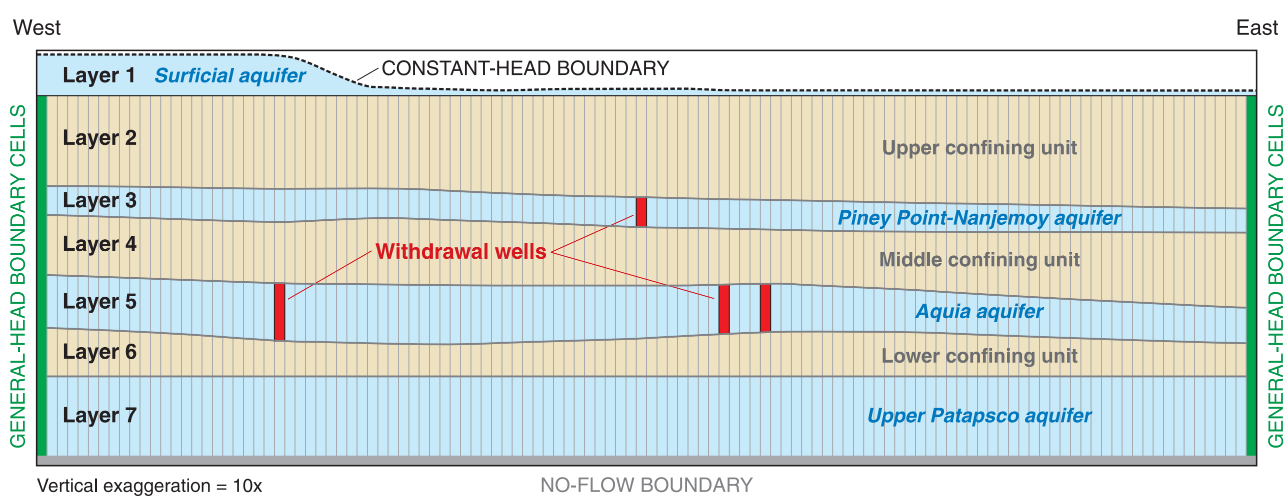

Figure 6. Diagram of model layering, vertical discretization, and boundary conditions along row 60 (see figure 5).

The general head-boundary conductance (C) for each layer is the product of the horizontal hydraulic conductivity of the material (K_h) and the cross-sectional area (A) of the cell perpendicular to flow, divided by the distance between the specified head and the general-head boundary cell (L). The values used to calculate C and the resulting C values used in the transient and steady-state models are shown in table 3. The cross-sectional area (A) is calculated by multiplying the width of the cell (250 ft for all cells and all layers) by an average thickness for each layer. The L for each general-head boundary cell is 125 ft. The resulting C value remains constant through all stress periods (table 3).

Model Hydraulic Properties

Hydraulic properties input into the model include initial heads, vertical and horizontal hydraulic conductivities, and withdrawal data. The input values and the heads that are calculated for the model are average values for each 1.4-acre cell. Recharge is not explicitly modeled because layer 1 has a constant-head boundary condition.

The initial heads for the transient model represent pre-stressed conditions. The initial head values for the Upper Patapsco, Aquia, and Piney Point-Nanjemoy aquifers were based on pre-pumping conditions simulated by Fleck and Vroblesky (1996, pls. 1, 5, and 6). The initial heads for the surficial aquifer ranged from 0.5 to 91 ft and were determined by adjusting the topography by an approximate thickness of the unsaturated zone. Limited data exist for head values in the confining units, therefore the initial heads for the confining unit model layers were calculated as a mean value of the heads in the aquifer layers adjacent to the confining unit layers. Constant values of 7, 8, 10, 12, 18, and 25 ft were used for the initial heads for layers 2 through 7, respectively.

Initial K_h values were estimated from previously published specific capacity, transmissivity, or hydraulic conductivity values. Calibrated K_h values for the aquifer model layers range from 10 to 20 ft/d; K_h for the confining units is 0.0002 ft/d (table 2).

Few vertical hydraulic conductivity (K_v) values have been reported in the literature. When available, these values were used for initial K_v input values. Calibrated K_v values in the model range from 1 to 2 ft/d for aquifer layers and a value of 0.00002 ft/d was used for all confining units (table 2); these values are one order of magnitude less than the K_h of the respective layer.

The transient ground-water-flow model simulates the period from 1900 (unstressed) through 2002. The time is discretized into 106 stress periods and subdivided into 161

Table 2. Ground-water-flow model input values.

[ft, feet; ft/d, feet per day]

Hydrogeologic Unit	Layer number	Model layer thickness, in ft	Horizontal hydraulic conductivity, in ft/d	Vertical hydraulic conductivity, in ft/d
Surficial aquifer	1	10–101	10	1
Upper confining unit	2	190–265	0.0002	.00002
Piney Point-Nanjemoy aquifer	3	45–75	10	1
Middle confining unit	4	123–185	.0002	.00002
Aquia aquifer	5	70–144	15	1.5
Lower confining unit	6	45–120	.0002	.00002
Upper Patapsco aquifer	7	200	20	2

Table 3. Values used to calculate general-head boundary conductance values, and resulting general-head boundary conductance values.

[ft, feet; ft/d, feet per day; ft^2/d, feet squared per day]

Layer	Horizontal hydraulic conductivity (K_h), in ft/d	Cell width (W), in ft	Average cell thickness (b), in ft	Distance (L), in ft	Calculated conductance value (C), in ft^2/d
2	0.0002	250	230	125	0.092
3	10	250	65	125	1260
4	0.0002	250	150	125	0.060
5	15	250	110	125	3360
6	0.0002	250	90	125	0.036
7	20	250	200	125	7980

time steps varying in length from multiple years to 7 days. Withdrawal data were obtained from several sources (Klohe and Feehley, 2001, table 3; Achmad and Hansen, 1997, Appendices D, E; C. I. Frederick, Jr., Jahn Corporation, NAS Patuxent River, written commun., 2003) and input to the model for each of the 106 stress periods. The locations of the Piney Point-Nanjemoy and Aquia withdrawal wells used in the model are shown in figure 7. Ground-water withdrawal rates vary from stress period to stress period, but remain constant within each stress period of the transient model (table 4). The time span of each of the stress periods and the total daily withdrawal rate for the Piney Point-Nanjemoy and Aquia aquifers for each period are shown in table 4. Major withdrawals from these aquifers did not begin until the 1940s; therefore, there is no simulated withdrawal from any of the three aquifers until stress period three, which represents 1940 to 1950. Withdrawal from the Upper Patapsco production well at NAS Patuxent River began in November 2003, but the transient model simulation ended in December 2002, so withdrawal from the Upper Patapsco aquifer is not simulated.

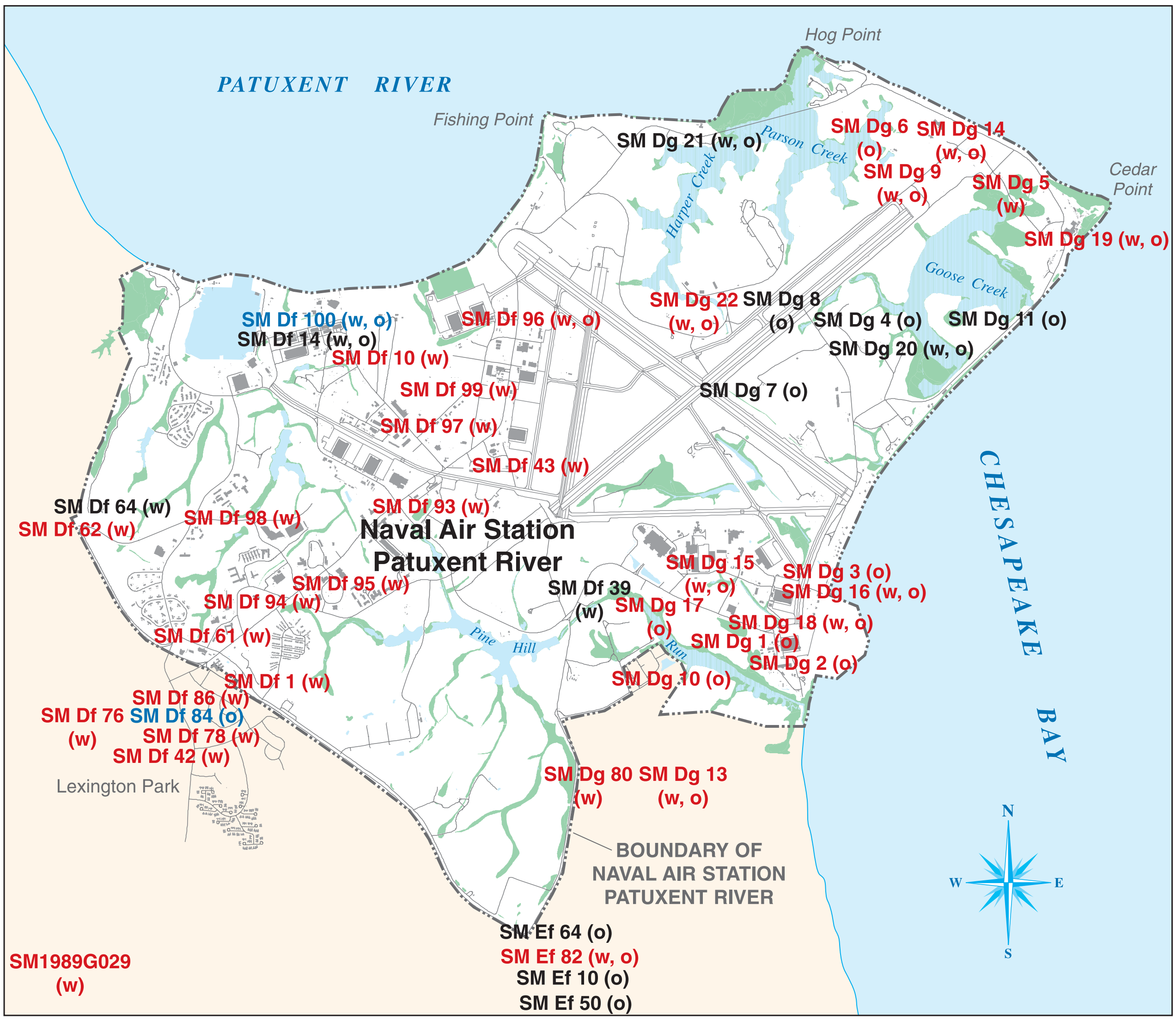

EXPLANATION

SM Ef 10	PINEY POINT-NANJEMOY AQUIFER WELL IDENTIFIER
SM Df 42	AQUIA AQUIFER WELL IDENTIFIER
SM Df 84	UPPER PATAPSCO AQUIFER WELL IDENTIFIER
(w)	WITHDRAWAL WELL
(o)	OBSERVATION WELL

Figure 7. Location of observation wells and withdrawal wells simulated in the transient ground-water-flow model at Naval Air Station Patuxent River, Maryland.

Table 4. Transient model stress periods with respective time periods and simulated withdrawal rates for the Piney Point-Nanjemoy aquifer, Aquia aquifer, and the stress period total, 1900–2002.

Stress period number	Time period	Withdrawal rate, in cubic feet per day		
		Piney Point-Nanjemoy aquifer	Aquia aquifer	Total
1	1900–1919	0	0	0
2	1920–1939	0	0	0
3	1940–1949	13,500	235,000	248,500
4	1950–1959	13,200	212,000	225,200
5	1960–1969	20,300	192,000	212,300
6	1970–1979	13,600	239,400	253,000
7	1980	11,200	222,000	233,200
8	1981	11,200	227,200	238,400
9	1982	11,200	236,200	247,400
10	1983	11,200	342,200	353,400
11	1984	11,200	242,400	253,600
12	1985	11,200	273,000	284,200
13	1986	11,200	273,000	284,200
14	1987	11,200	282,600	293,800
15	1988	11,200	301,200	312,400
16	1989	12	276,700	276,712
17	1990	12	239,600	239,612
18	1991	12	293,000	293,012
19	1992	12	257,670	257,682
20	1993	7,600	266,730	274,330
21	1994	23,600	259,200	282,800
22	1995	5,495	286,615	292,110
23	Jan. 1996	5,490	239,116	244,606
24	Feb.	7,130	241,691	248,821
25	Mar.	4,998	252,670	257,668
26	Apr.	6,174	256,834	263,008
27	May	496	250,689	251,185
28	June	7,359	252,687	260,046
29	July	9,830	244,464	254,294
30	Aug.	5,940	250,053	255,993
31	Sept.	7,487	244,967	252,454
32	Oct.	6,819	241,155	247,974
33	Nov.	6,199	237,112	243,311
34	Dec.	5,613	236,386	241,999
35	Jan. 1997	8,649	203,535	212,184
36	Feb.	11,185	217,262	228,447
37	Mar.	6,558	198,906	205,464
38	Apr.	16,629	232,877	249,506
39	May	4,202	207,608	211,810
40	June	19,451	222,240	241,691
41	July	8,484	235,055	243,539
42	Aug.	11,020	218,981	230,001
43	Sept.	8,421	212,656	221,077
44	Oct.	406	216,069	216,475
45	Nov.	171	219,256	219,427
46	Dec.	167	215,372	215,539
47	Jan. 1998	202	233,761	233,963
48	Feb.	157	233,129	233,286
49	Mar.	164	245,243	245,407
50	Apr.	363	240,123	240,486
51	May	186	249,375	249,561
52	June	347	245,005	245,352
53	July	321	256,745	257,066
54	Aug.	228	283,640	283,868
55	Sept.	159	283,736	283,895
56	Oct.	148	241,851	241,999

Table 4. Transient model stress periods with respective time periods and simulated withdrawal rates for the Piney Point-Nanjemoy aquifer, Aquia aquifer, and the stress period total, 1900–2002.—Continued

Stress period number	Time period	Withdrawal rate, in cubic feet per day		
		Piney Point-Nanjemoy aquifer	Aquia aquifer	Total
57	Nov.	131	232,465	232,596
58	Dec.	150	228,304	228,454
59	Jan. 1999	1,430	230,679	232,109
60	Feb.	686	236,863	237,549
61	Mar.	178	243,334	243,512
62	Apr.	1,318	245,742	247,060
63	May	3,669	245,258	248,927
64	June	7,018	251,004	258,022
65	July	10,676	252,428	263,104
66	Aug.	8,160	237,657	245,817
67	Sept.	4,961	222,988	227,949
68	Oct.	132	234,817	234,949
69	Nov.	58	215,970	216,028
70	Dec.	67	218,133	218,200
71	Jan. 2000	43	254,555	254,598
72	Feb.	38	251,575	251,613
73	Mar.	34	256,583	256,617
74	Apr.	56	246,418	246,474
75	May	71	246,776	246,847
76	June	87	253,090	253,177
77	July	84	243,123	243,207
78	Aug.	111	245,865	245,976
79	Sept.	122	244,200	244,322
80	Oct.	104	240,992	241,096
81	Nov.	94	235,725	235,819
82	Dec.	80	236,495	236,575
83	Jan. 2001	75	262,383	262,458
84	Feb.	153	249,678	249,831
85	Mar.	124	250,724	250,848
86	Apr.	134	257,012	257,146
87	May	134	279,652	279,786
88	June	147	271,475	271,622
89	July	323	275,575	275,898
90	Aug.	270	280,764	281,034
91	Sept.	345	273,468	273,813
92	Oct.	147	260,588	260,735
93	Nov.	253	255,065	255,318
94	Dec.	109	244,196	244,305
95	Jan. 2002	94	250,904	250,998
96	Feb.	96	254,164	254,260
97	Mar.	121	257,998	258,119
98	Apr.	135	261,096	261,231
99	May	244	277,129	277,373
100	June	252	301,923	302,175
101	July	194	303,796	303,990
102	Aug.	195	301,854	302,049
103	Sept.	201	277,495	277,696
104	Oct.	174	269,657	269,831
105	Nov.	166	260,376	260,542
106	Dec.	239	260,800	261,039

Model Calibration

Initial heads, and horizontal and vertical hydraulic conductivity of the aquifers and confining beds were adjusted using trial-and-error methods to calibrate the transient ground-water-flow model. The model was considered calibrated when the simulated water-level trends matched the observed water-level trends, the error between the observed (or measured) water levels and the simulated water levels was minimized, and the input parameters, water budgets, and simulated flow directions were reasonable. The well locations for which water-level observations were available for model calibration are shown in figure 7. A total of 27 wells were used in model calibration (10 screened in the Piney Point-Nanjemoy aquifer, 15 screened in the Aquia aquifer, and 2 screened in the Upper Patapsco aquifer). The root-mean-squared error (RMSE) was used to calculate the error between the observed and simulated water levels. The RMSE is equal to the average of the squared differences in measured and simulated water levels (Anderson and Woessner, 1992). Simulated water levels from the transient model were generally consistent with observed water levels. A hydrograph of observed and simulated water levels for well SM Dg 21 screened in the Piney Point-Nanjemoy aquifer is shown in figure 8. The RMSE for Piney Point-Nanjemoy well SM Dg 21 was 1.19 ft (table 5).

Hydrographs of observed and simulated water levels for wells (SM Df 1, SM Df 61, SM Df 80, SM Df 95, SM Dg 10, and SM Dg 14) screened in the Aquia aquifer are shown in figure 9. The simulated water levels generally agree with the observed values and closely match the downward trend of water levels in the observation wells. RMSE values for wells screened in the Aquia aquifer range from 5.9 to 11 ft, with a mean of 7.7 ft (table 5). The RMSE for SM Df 61 (10.98 ft) is skewed by two observations that likely reflect short-term withdrawals not accounted for in the transient model. If those two observations are not used in the RMSE calculation, the RMSE is approximately 7 ft, rather than 11 ft.

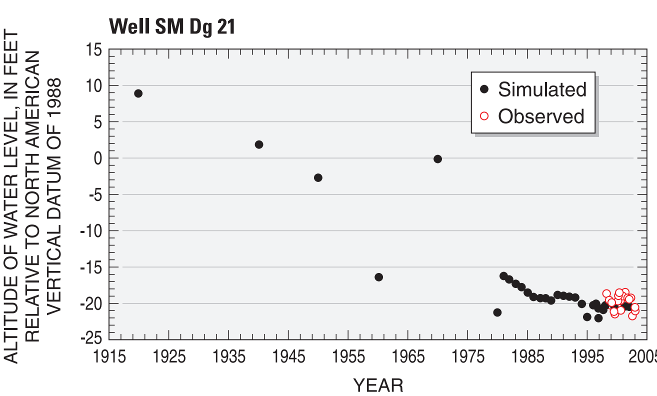

Figure 8. Observed and model-simulated hydrographs for well SM Dg 21 screened in the Piney Point-Nanjemoy aquifer from the transient simulation. (Well locations shown in figure 7.)

Table 5. Root-mean-squared-error (RMSE) values for the transient ground-water-flow model simulation.

[USGS, U.S. Geological Survey]

USGS well number	Aquifer (model layer)	RMSE, in feet
SM Dg 21	Piney Point-Nanjemoy aquifer (3)	1.19
SM Df 1	Aquia aquifer (5)	7.45
SM Df 61	Aquia aquifer (5)	10.98
SM Df 80	Aquia aquifer (5)	5.90
SM Df 95	Aquia aquifer (5)	6.08
SM Dg 10	Aquia aquifer (5)	7.30
SM Dg 14	Aquia aquifer (5)	8.27
SM Df 84	Upper Patapsco aquifer (7)	2.42
SM Df 100	Upper Patapsco aquifer (7)	1.69

Two wells screened in the Upper Patapsco aquifer (SM Df 84 and SM Df 100) were used to calibrate model layer 7. Hydrographs of observed and simulated water levels for wells SM Df 84 and SM Df 100 are shown in figure 10. The simulated water levels agree with the observed water levels and closely match the downward trend of water levels in the observation wells. The RMSEs for wells SM Df 84 and SM Df 100 are 2.42 and 1.69 ft, respectively.

Model Sensitivity

In addition to checking model calibration, it is also important to test the sensitivity of the model to changes in model input parameters. The sensitivity analysis helps quantify the uncertainty of the calibrated model due to uncertainty in model input parameters, stresses, and boundary conditions (Anderson and Woessner, 1992). By systematically changing one input parameter at a time, the effects of the input parameter on the model-simulated heads and flow can be evaluated. The sensitivity analysis indicates which input parameters impact the ability of the model to match observed values (Reilly and Harbaugh, 2004).

A sensitivity analysis was performed on the calibrated model under steady-state conditions (December 2002 simulation) by systematically changing the K_h of selected layers (while keeping K_v constant and therefore changing the K_h to K_v ratio), the K_h and K_v of selected layers (keeping the K_h to K_v ratio constant), the general-head boundary conductance values, and the withdrawal rates. In each simulation, one parameter was changed by increasing the parameter by one and two orders of magnitude and then decreasing the parameter by one and two orders of magnitude. The steady-state simulated water levels were compared to the observed water levels for each sensitivity analysis simulation. The RMSE was calculated for 18 wells (1 Piney Point-Nanjemoy aquifer well, 6 Aquia aquifer wells, and 2 Upper Patapsco aquifer wells) for

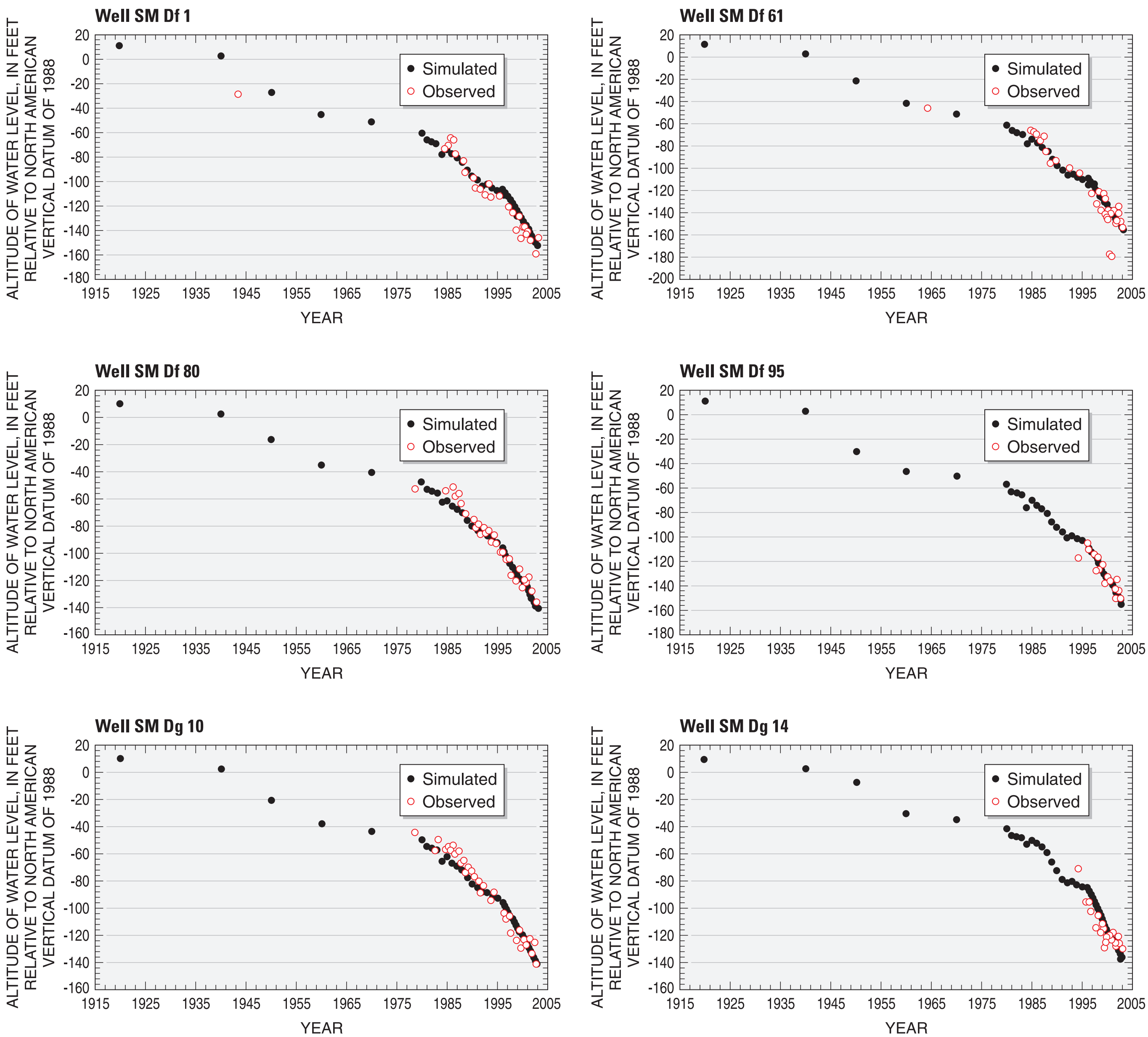

Figure 9. Observed and model-simulated hydrographs for six wells screened in the Aquia aquifer from the transient simulation. (Well locations shown in figure 7.)

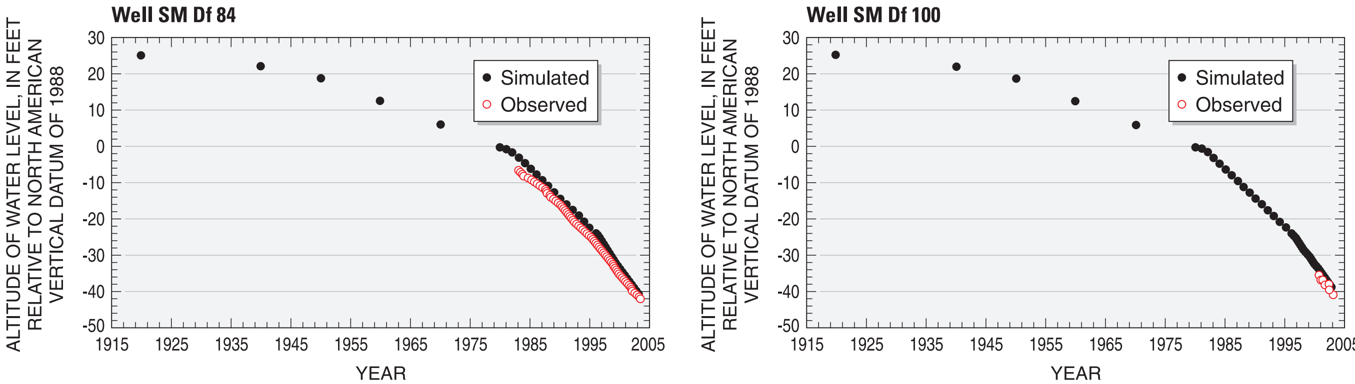

Figure 10. Observed and model-simulated hydrographs for two wells screened in the Upper Patapsco aquifer from the transient simulation. (Well locations shown in figure 7.)

each sensitivity analysis simulation to compare the observed water levels to the simulated water levels.

The sensitivity analysis indicates that the model-simulated water levels are most sensitive to decreases in the $K_{h,}$ and large decreases (two orders of magnitude) in general-head boundary conductance (fig. 11). The model-simulated water levels are also sensitive to increases in withdrawal rates, and the two orders-of-magnitude increase in the K_h and K_v of the confining units (layers 2, 4, and 6).

Model-simulated water levels were least sensitive to increases or decreases in the K_h of the upper and middle confining units, decreases in K_h and K_v of all confining units, decreases in withdrawal rates, increases or decreases in K_h of layer 3, increases in general-head boundary conductance, or increases in the K_h of layer 5 (fig. 11). The sensitivity analysis is limited because it was conducted on the steady-state simulation. Thus, the sensitivity of the model to changes in the storage coefficient could not be tested.

The sensitivity analysis also demonstrates the appropriateness of using the general-head boundary for the model boundary conditions. When using a general-head boundary, it is important to use an appropriate head value and conductance value. If the general-head boundary conductance is too high, the general-head boundary will act like a constant-head boundary, causing water levels in the boundary cells to remain constant even when stresses, such as withdrawal rates, increase. In contrast, if the general-head boundary conductance is too low, the general-head boundary will act like a no-flow boundary, causing greater drawdowns than would realistically be expected when stresses increase. For this model, an appropriate general-head boundary conductance is necessary so that the boundary does not act like either a constant head boundary or a no-flow boundary; that is, both water levels and fluxes should change when model stresses change, since the stresses are near the boundary. As the general-head boundary conductance increases, the RMSE does not change (fig. 11), and as the general-head boundary conductance decreases by two orders of magnitude, the RMSE increases dramatically, indicating that the general-head boundary begins to act like a no-flow boundary (fig. 11). The sensitivity analysis of the general-head boundary conductance indicates that within the range of values used, the general-head boundary was appropriate.

Model Limitations

The model is limited by the validity of the conceptual model, the design of the ground-water-flow model, and the accuracy of the input parameters. Specific issues and assumptions that may limit the model include: (1) the model was designed to simulate ground-water levels and fluxes in the aquifers beneath the NAS Patuxent River. The model was calibrated to water levels measured at the NAS Patuxent River, and nearby monitoring wells. If the model area is increased, re-calibration would be necessary; (2) the model assumes that the no-flow boundary between the Upper Patapsco aquifer and the confining unit below is a reasonable representation; however, given the complex nature of the fluvial sediments of the Patapsco Formation, if leakage to or from the deeper aquifers does occur, it is not accounted for in the model; (3) the model assumes that the surficial aquifer water levels are constant over time and mimic land-surface elevations; (4) the model assumes that using an average K_h is appropriate. In reality, there are likely heterogeneities in hydraulic conductivities; and (5) the model assumes that withdrawal rates outside the main air station are accounted for in the heads of the general-head boundaries, or they are far enough outside the model boundary so that they do not affect the modeled area.

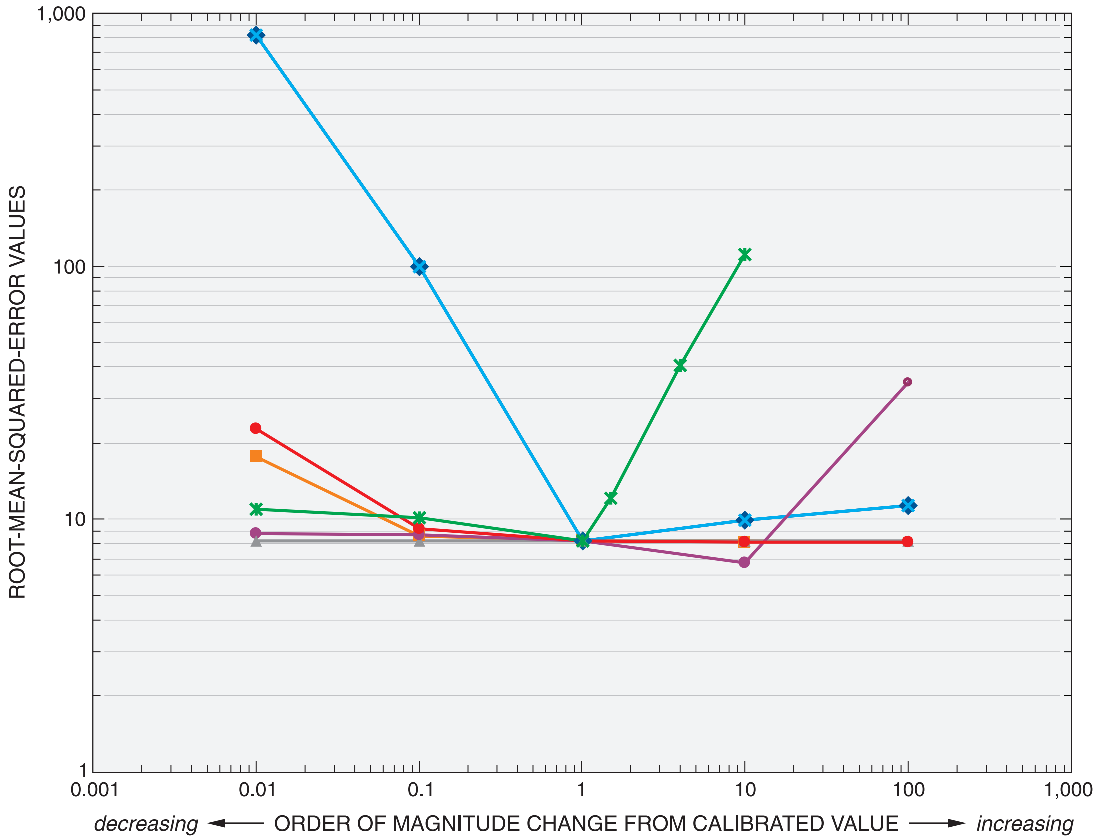

EXPLANATION

- Horizontal hydraulic conductivity (K_h) of layer 5 (Aquia aquifer) [Vertical hydraulic conductivity (K_v) was constant, such that K_h:K_v was not held constant.]
- Horizontal hydraulic conductivity of layer 3 (Piney Point-Nanjemoy aquifer) (K_h:K_v not constant)
- Horizontal hydraulic conductivity of layers 4 and 6 (upper and middle confining units) (K_h:K_v not constant)
- Horizontal and vertical hydraulic conductivity of layer 5 (Aquia aquifer) (Horizontal and vertical hydraulic conductivity of layer 5 were changed, such that K_h:K_v was constant.)
- Horizontal and vertical hydraulic conductivity of layers 2, 4, and 6 (upper, middle, and lower confining units) (K_h:K_v constant.)
- Conductance of general-head boundary cells
- Withdrawal rates

Figure 11. Results of the steady-state ground-water-flow model sensitivity analysis showing root-mean-squared-error (RMSE) values for the sensitivity-analysis simulations.

Water Budget

The water budget of the ground-water-flow model describes the sources and sinks of ground water in the flow system. The overall water budget for stress period 106, time step 4 of the transient simulation, which represents December 2002 conditions, is shown in table 6. The results of the simulation indicate that there are three inflows of water into the modeled system: general head boundaries, storage, and constant head cells. Ninety-seven percent of the inflow is through the general-head boundaries, 2 percent is from storage, and 1 percent is through the constant-head cells. Flows out of the modeled system are through pumping wells and general-head boundaries. The pumping wells account for 64 percent of the outflow, and the general-head boundaries account for the other 36 percent.

A more detailed budget analysis of the part of the Piney Point-Nanjemoy, Aquia, and Upper Patapsco aquifers that underlie the main air station is summarized in figure 12. The schematic shows net flows in and between the model layers for model stress periods 2, 22, and 106 from the transient model, which represent simulations of the periods 1920–1940, 1995, and December 2002, respectively. For this analysis, the net inflows and outflows, or net water budgets, are subdivided into 3 zones within each model layer: the area on the land side of the main air station, the area directly underlying the main air station, and the shore side of the main air station (figure 5). Net flows directly from the land side of the main air station to the shore side of the main air station are not shown in figure 12.

The simulated net inflows and outflows for the period 1920 to 1940 represent pre-pumping conditions in the aquifer system. There are no simulated withdrawals from any of the aquifers. There is minimal flow vertically between the aquifers and confining units. For the Piney Point-Nanjemoy and Aquia aquifers, the net flow is from the land side of the main air station to the shore side of the main air station. In the Patapsco aquifer, the net flow is from the shore side of the main air station to the land side (fig. 12).

Between 1940 and 1995, there were many changes in the simulated net inflows and outflows as withdrawals of the Piney Point-Nanjemoy and Aquia aquifers began and continued to increase. In 1995, the rate of withdrawal from the Piney Point-Nanjemoy aquifer was 5.5 x 10^3 ft^3/d (cubic feet per day) and the withdrawal rate from the Aquia aquifer was 98 x 10^3 ft^3/d. This caused the hydraulic gradients to change the net flow directions in both aquifers to be towards the area underlying the base from both the land side and the shore side of the main air station. All of the net vertical flows increased to accommodate the large increase in withdrawal from the Aquia aquifer. The magnitude of the net horizontal flow also increased by as much as 35 times the amount simulated in 1940 (fig. 12).

Between 1995 and 2002, the rate of withdrawal from the Piney Point-Nanjemoy aquifer decreased from 5.5 x 10^3 ft^3/d to 0.2 x 10^3 ft^3/d, and the rate of withdrawal from the Aquia aquifer decreased from 98 x 10^3 ft^3/d to 90 x 10^3 ft^3/d (fig. 12). The decrease in withdrawal rates decreases the net flow from the shore side to the area underlying the main air station from all three aquifers. The net vertical flows to the Aquia aquifer from the lower and middle confining units were slightly higher in 2002 than in 1995 (fig. 12).

The Upper Patapsco aquifer was not pumped within the model area through the end of 2002. The net flux into and out of the Upper Patapsco is controlled either by withdrawal upgradient from the model area, or flows vertically up through the lower confining unit to the Aquia aquifer. The upgradient withdrawals are represented in the model by the changing potentiometric surfaces used to calculate the specified heads for the general-head boundaries for the transient simulation. Large regional increases in ground-water withdrawal, likely from both the Upper Patapsco and Aquia aquifers, from 1940 to 1995 and 2002 have increased the net rate of flow through the Upper Patapsco aquifer that underlies the NAS Patuxent River, as shown in figure 12.

Table 6. Water budget for the entire model domain for stress period 106 (December 2002) of the transient model.

[ft^3/d, cubic feet per day]

Inflows			Outflows		
Component	**ft^3/d**	**percent**	**Component**	**ft^3/d**	**percent**
Storage	9,843	2	Storage	0	
Constant-head boundaries	2,746	1	Constant-head boundaries	0	
Wells	0		Wells	261,039	64
General-head boundaries	393,041	97	General-head boundaries	144,591	36
Total	**405,631**	**100**	**Total**	**405,630**	**100**
Total inflows - outflows	**1**				

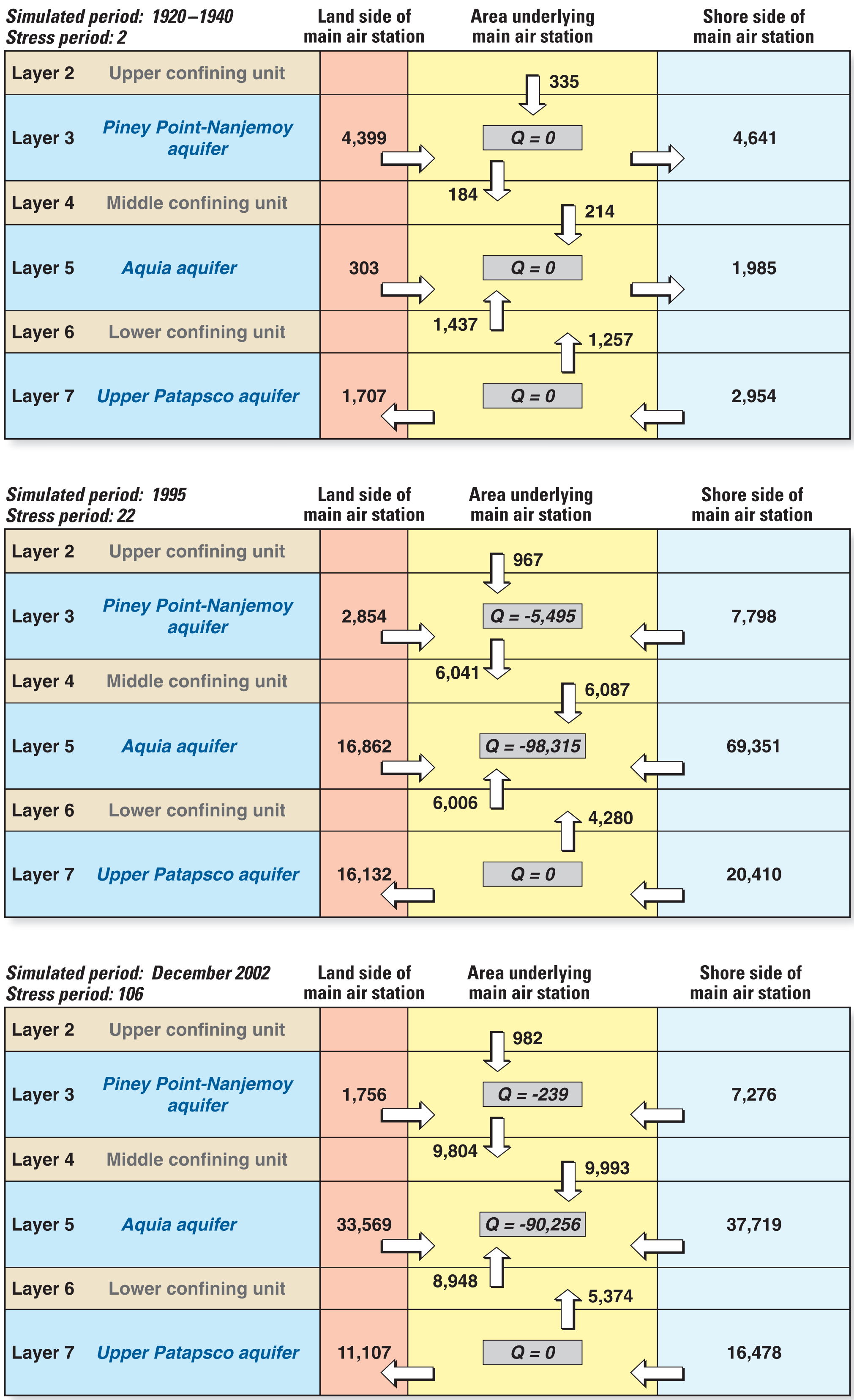

Figure 12. Simulated net inflows and outflows, in cubic feet per day, for the parts of the Piney Point-Nanjemoy, Aquia, and Upper Patapsco aquifers that underlie the Naval Air Station Patuxent River. (Negative values indicate flow out of the model.)

Optimization Model

Optimization modeling of aquifer systems links ground-water-flow models with optimization methods. This approach allows the development of optimization strategies that optimize ground-water utilization while minimizing aquifer stress to be tested (Barlow, 2005). Deninger (1970) was the first to use the combination of a ground-water-flow model and optimization methods for the management of water resources. He developed an optimization model to maximize water withdrawals from a well field subject to certain limitations on drawdown. Since Deninger's approach was developed, there have been over 100 studies in which ground-water-flow and optimization models were combined to manage the ground-water resource (Gorelick, 1983; Wagner, 1995; Banks and Dillow, 2001; Czarnecki and others, 2003; Granato and Barlow, 2005; Andreasen, 2007).

There are four main components of an optimization model. The first component is defining the objective function. Typical objective functions for optimization models include minimizing well construction or pumping costs, maximizing water withdrawals, or minimizing hydrologic impacts. The second component is defining the constraints of the optimization model. Several types of constraints may be specified, including hydrogeologic, withdrawal (balance), integer, and withdrawal-rate bounds. A combination of constraints may need to be used in order to achieve the goal of the objective function, and to avoid non-uniqueness of an optimization model. The third component is defining the decision variables. The decision variables describe the parameters that control the solution to the optimization model. The fourth component is to develop the formulation statement. The formulation statement combines all of the other three components by relating the objectives of the design, the constraints of the design, and the goals of the design to each other (Ahlfeld and Mulligan, 2000).

Linear optimization software translates the formulation statement into mathematical equations that are solved to determine the optimal solution. A response matrix method is used to transform the optimization problem into a linear or mixed integer formulation that is written into an ASCII file in MPS (Mathematical Programming System) format. The MPS file is read into the linear optimization software that generates a file that contains the optimal solution. The solution is translated back to a form that can be read by the ground-water modeling software. For the optimization models developed for the NAS Patuxent River and discussed later in this report, LINDO (Schrage, 1997; HyperLINDO/PC, 1998; Lindo Systems, Inc., 2001) is used to solve the objective function formulation, and then MODMAN (MODFLOW MANagement) (Greenwald, 1998a, 1998b) interfaces between LINDO and MODFLOW.

Response Function

The concept and use of the response function is critical to the implementation of the linear or mixed integer optimization programming methodology. Linear response theory in confined ground-water-flow systems, such as the one that underlies NAS Patuxent River, is based on the principle of linear superposition. This theory specifies first, that an increase in the withdrawal rate by a factor increases drawdown at any given cell by the same factor and second, that drawdown induced by withdrawal from more than one well is equal to the sums of drawdown induced by the withdrawal from each individual well (Greenwald, 1998a). Linear superposition is applicable to both the transient and the steady-state versions of the NAS Patuxent River ground-water-flow model.

Coefficients are calculated at each well by applying a withdrawal rate and then determining the drawdown at each control location. This withdrawal rate is referred to as the unit stress or unit rate. The drawdown response at each control location is equal to the unmanaged head minus the head resulting from the unit rate. The unit response is equal to the drawdown response divided by the unit rate. This is the drawdown resulting from a rate of one unit. Thus, the drawdown due to the actual withdrawal, which is referred to as the induced drawdown, is equal to the unit response times the well rate.

Application

Two hypothetical optimization scenarios were designed and evaluated for NAS Patuxent River. The optimization model was based on a steady-state simulation of December 2002 conditions (withdrawals and general-head boundary heads) using the calibrated model. The overall goals of the optimization model were to (1) demonstrate the potential utility of optimization models, and (2) optimize ground-water withdrawals for two scenarios at NAS Patuxent River given specific constraints while minimizing drawdown in the Aquia aquifer at Lexington Park. The objective of the first scenario was to optimize the withdrawal from wells, while minimizing the drawdown in the local potentiometric surface of the Aquia aquifer. The objective of the second scenario was to determine the optimal location for a hypothetical new well for increased withdrawals in the eastern-northeastern part of the main air station while minimizing the drawdown at control nodes along the western boundary of the main air station.

Scenario 1: Minimize Drawdown of Local Heads

The objective of this scenario was to optimize the withdrawal from three groups of main air station wells, while minimizing the drawdown in the local potentiometric surface of the Aquia aquifer. The objective was achieved by minimizing drawdown at a control node (row 67, column 22) (figs. 5 and 13) in layer 5 (Aquia aquifer) located at the western edge of the base and adjacent to St. Mary's Metropolitan Commission production wells at Lexington Park.

The constraints specified included three types—hydrogeologic, balance, and withdrawal-rates bounds. At the control node location, a hydrogeologic constraint of 10 ft of drawdown was set as the maximum limit. The other two types of constraints are discussed below.

There are two types of production wells at the NAS Patuxent River. The bulk of the production is from 15 wells that are separated into three groupings, which operate as individual units. These groupings are referred to as the "A," "B," and "C" groups (fig. 13, table 7) and their rates will be managed by the optimization model. Another eight production wells are sole-source, site-specific wells and are required to pump a specific amount of water. Withdrawals from these eight wells, and nine wells located off the main air station in Lexington Park, were not optimized by the model. Withdrawals from these unmanaged wells totaled 178,379 ft^3/d (table 8).

Balance constraints were applied to the three production well groupings. The air station continues to be a receiver base as a result of BRAC, with workforce population potentially increasing by 9,000 above the 2002 population of 19,000. This workforce population increase results in an increased demand for water. For this scenario, it was assumed that this is a 25-percent increase above the 2002 production levels for each of the three production well groups. Thus, this would be a balance constraint of 34,000; 59,000; and 26,000 ft^3/d for the A, B, and C groups, respectively (fig. 13). Total withdrawals from the three groups at the main air station are 119,000 ft^3/d (table 7).

Two types of withdrawal-rate-bounds constraints were applied to all 15 managed wells. It was assumed, for this scenario, that for maintenance purposes, each of the 15 wells needed to be pumped at an average minimum rate of 1,000 ft^3/d. A maximum withdrawal constraint was also set for each managed well. This rate was determined by increasing the maximum average monthly rate for the period 1995–2002 by 10 percent. The maximum withdrawal constraint for each well is shown in table 7.

The optimization algorithm of the LINDO program calculated that pumping the managed wells at the rates shown in table 7 and figure 14 attains a minimum drawdown for the control node of 5.7 ft. Four of the managed wells are pumped at maximum capacity, another two are pumped at lower rates, and the other nine are pumped at the minimum rate necessary for pump maintenance. The unmanaged wells were pumped at the December 2002 rate (table 8). The optimization program calculated that the minimum drawdown caused by a 25-percent increase in withdrawals over the December 2002 rates from the managed wells was 5.7 ft at the control location.

Scenario 2: Locate a Second Well for the Northeast Area in the Aquia Aquifer

In this scenario, an optimal location resulting in the least amount of drawdown at eight control node locations for a second Aquia aquifer well in the northeast part of NAS Patuxent River near production well SM Dg 19 was selected. The optimized location resulted in the least amount of drawdown at the eight control nodes.

In scenario 1, three well groupings were optimized to accommodate a possible increase in base withdrawals at the NAS Patuxent River (fig. 13). The well groupings are in the central and western parts of the main air station. Well withdrawals in the northeast part of the main air station were not optimized. In this scenario, there is a hypothetical need for an increased total withdrawal of 66,800 ft^3/d in the northeast part of the main air station. For this scenario, well SM Dg 19 is pumped at 33,400 ft^3/d, half of the hypothetical withdrawal of 66,800 ft^3/d. For the period 1995 through 2002, the maximum average monthly pumping rate for SM Dg 19 was 23,797 ft^3/d. The optimization program was used to determine the best location of a second well also pumping at 33,400 ft^3/d and located near well SM Dg 19 so that the wells could be tied to the same distribution system. Ten candidate locations near well SM Dg 19 were distributed in an approximate circle around well SM Dg 19, as shown in figure 15. The management model was used to determine which of these sites produced the least amount of drawdown at the eight control nodes located along the western boundary of the main air station (fig. 15).

The well-rate-bound and drawdown constraints from scenario 1 were used in this scenario. Additionally, seven more drawdown constraint nodes were added to the problem. These control nodes are located outside the perimeter of the main air station (fig. 15). The candidate well locations were specified with head limits, where the heads in the cells cannot fall below the top of the aquifer (approximately 375 ft below sea level).

The optimal location for the additional well is also shown in figure 15. The effect of the additional well and well SM Dg 19 (pumping at a combined rate of 66,800 ft^3/d), an increase of 43,000 ft^3/d above the rate well SM Dg 19 alone withdrew, resulted in an additional drawdown of about 0.2 ft at the control node location that was used in both scenarios. Predicted drawdown at well SM Dg 19 due to the combined withdrawal at well SM Dg 19 and the additional well was about 49 ft.

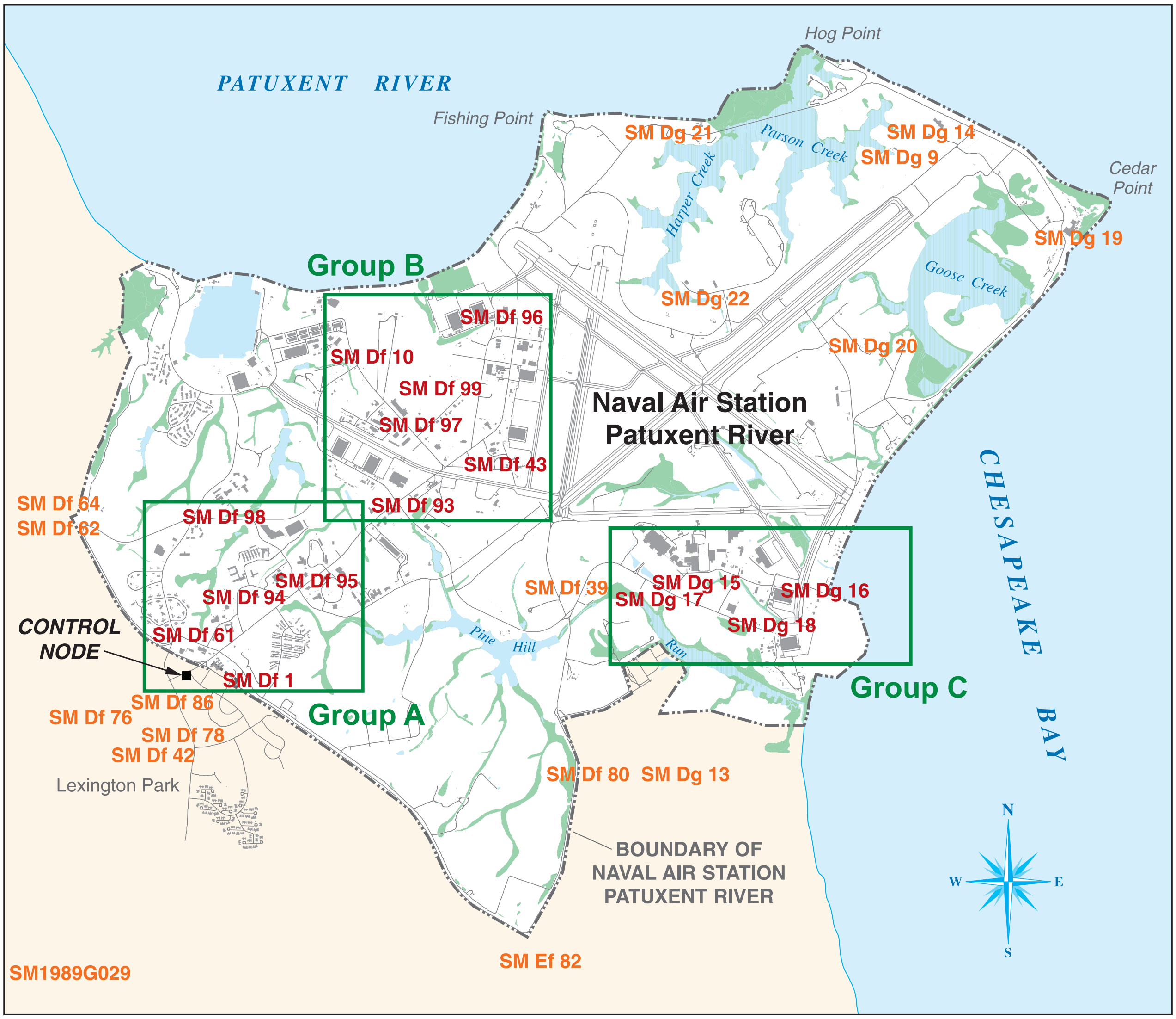

EXPLANATION

SM Df 97 WELL IDENTIFIER–MANAGED

SM Df 76 WELL IDENTIFIER–UNMANAGED

■ CONTROL NODE LOCATION

Group A	Group B	Group C
Q_{2002} = 27,000 cubic feet per day (ft^3/d)	Q_{2002} = 47,000 ft^3/d	Q_{2002} = 21,000 ft^3/d
$Q_{2002\,+\,25\%}$ = 34,000 ft^3/d	$Q_{2002\,+\,25\%}$ = 59,000 ft^3/d	$Q_{2002\,+\,25\%}$ = 26,000 ft^3/d

Figure 13. Groupings of wells (A, B, and C) screened in the Aquia aquifer and control node for hypothetical optimization scenario 1 at the Naval Air Station Patuxent River, Maryland.

Table 7. Hypothetical scenario 1: optimization model managed wells, steady-state ground-water-flow model withdrawal rates, and optimal withdrawal rates from the optimization model.

[USGS, U.S. Geological Survey; ft^3/d, cubic feet per day]

USGS well number	Row	Column	Layer	Group	Steady-state model withdrawal rate, in ft^3/d	Maximum withdrawal constraint rate, in ft^3/d	Optimal optimization model withdrawal rate, in ft^3/d
SM Df 98	52	22	5	A	10,369	29,400	29,400
SM Df 95	59	33	5	A	9,117	23,500	1,600
SM Df 1	69	26	5	A	1,055	13,000	1,000
SM Df 61	64	19	5	A	5,916	10,700	1,000
SM Df 94	60	24	5	A	397	17,900	1,000
Total					**26,854**	**94,500**	**34,000**
SM Df 96	32	50	5	B	13,847	38,500	38,000
SM Df 10	36	37	5	B	2,378	14,900	14,900
SM Df 99	39	44	5	B	9,050	12,700	3,100
SM Df 43	47	51	5	B	2,227	9,700	1,000
SM Df 93	51	41	5	B	13,562	38,700	1,000
SM Df 97	43	42	5	B	5,444	13,400	1,000
Total					**46,508**	**127,900**	**59,000**
SM Dg 16	57	83	5	C	12,499	27,900	23,000
SM Dg 17	60	67	5	C	2,833	10,600	1,000
SM Dg 15	60	71	5	C	2,792	16,000	1,000
SM Dg 18	63	77	5	C	2,998	22,000	1,000
Total					**21,122**	**76,500**	**26,000**

Table 8. Hypothetical scenario 1: optimization model unmanaged wells, steady-state ground-water-flow model withdrawal rates, and withdrawal rates for the optimization model.

[USGS, U.S. Geological Survey; ft^3/d, cubic feet per day]

USGS well number	Row	Column	Layer	Optimization model and steady-state model withdrawal rate, in ft^3/d
SM Df 39	60	59	3	57
SM Df 42	76	15	5	17,887
SM Df 62	53	3	5	69,545
SM Df 64	51	9	3	15
SM Df 76	72	9	5	19,866
SM Df 78	74	18	5	13,903
SM Df 80	78	61	5	6,254
SM Df 86	71	17	5	33,783
SM Dg 9	15	90	5	6,122
SM Dg 13	78	65	5	7,660
SM Dg 14	13	93	5	1,222
SM Dg 19	24	108	5	457
SM Dg 20	35	87	3	13
SM Dg 21	14	68	3	91
SM Dg 22	30	74	5	128
SM Ef 82	97	54	5	1,243
SM1989G029	97	5	5	133
Total				**178,379**

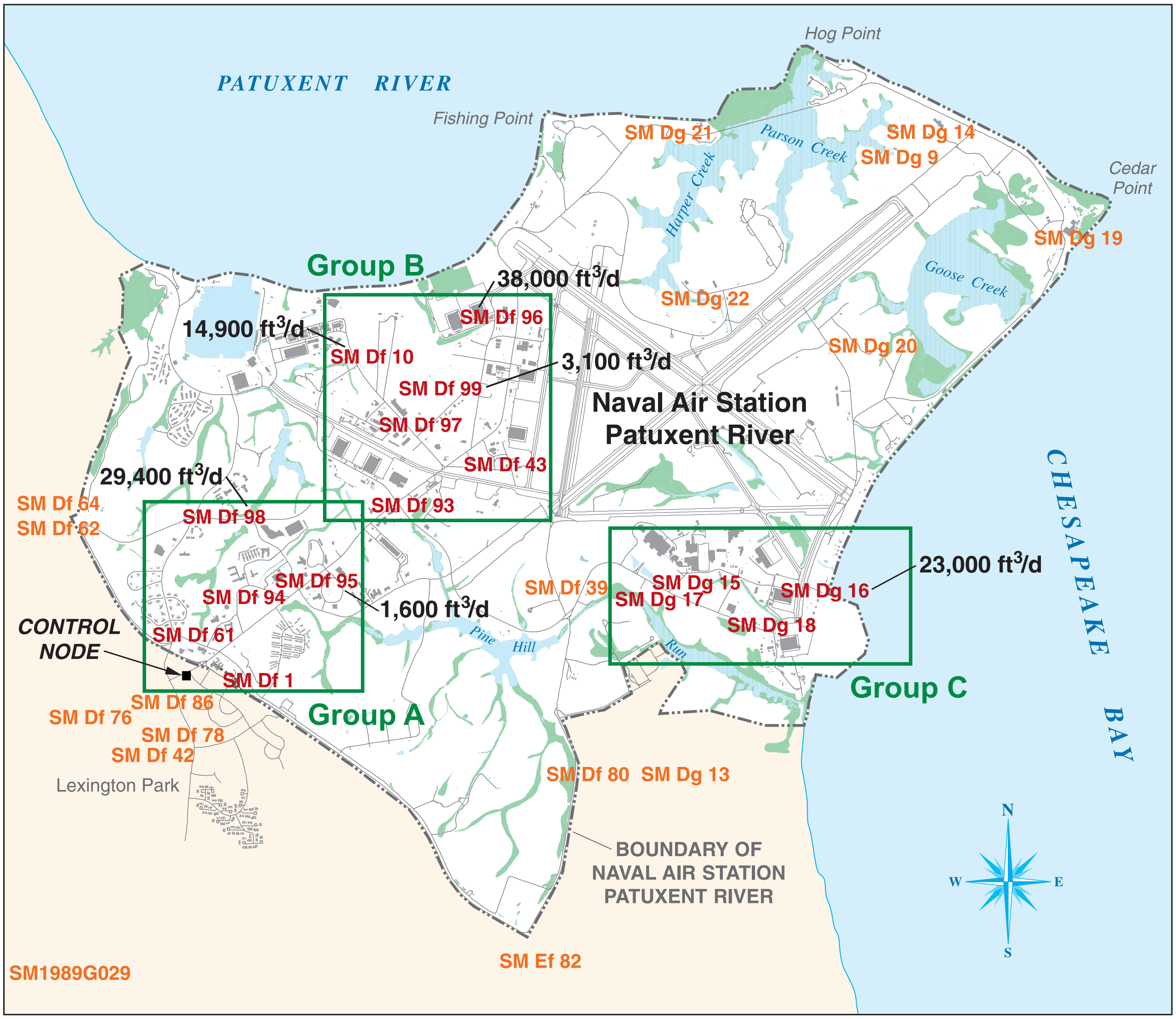

EXPLANATION

SM Df 97 WELL IDENTIFIER–MANAGED

SM Df 76 WELL IDENTIFIER–UNMANAGED

■ CONTROL NODE LOCATION

Figure 14. Optimal solution for hypothetical optimization scenario 1 at Naval Air Station Patuxent River, Maryland. [The number next to wells is the optimized withdrawal rate in ft³/d (cubic feet per day). The optimized withdrawal rate at all other managed wells is 1,000 ft³/d.]

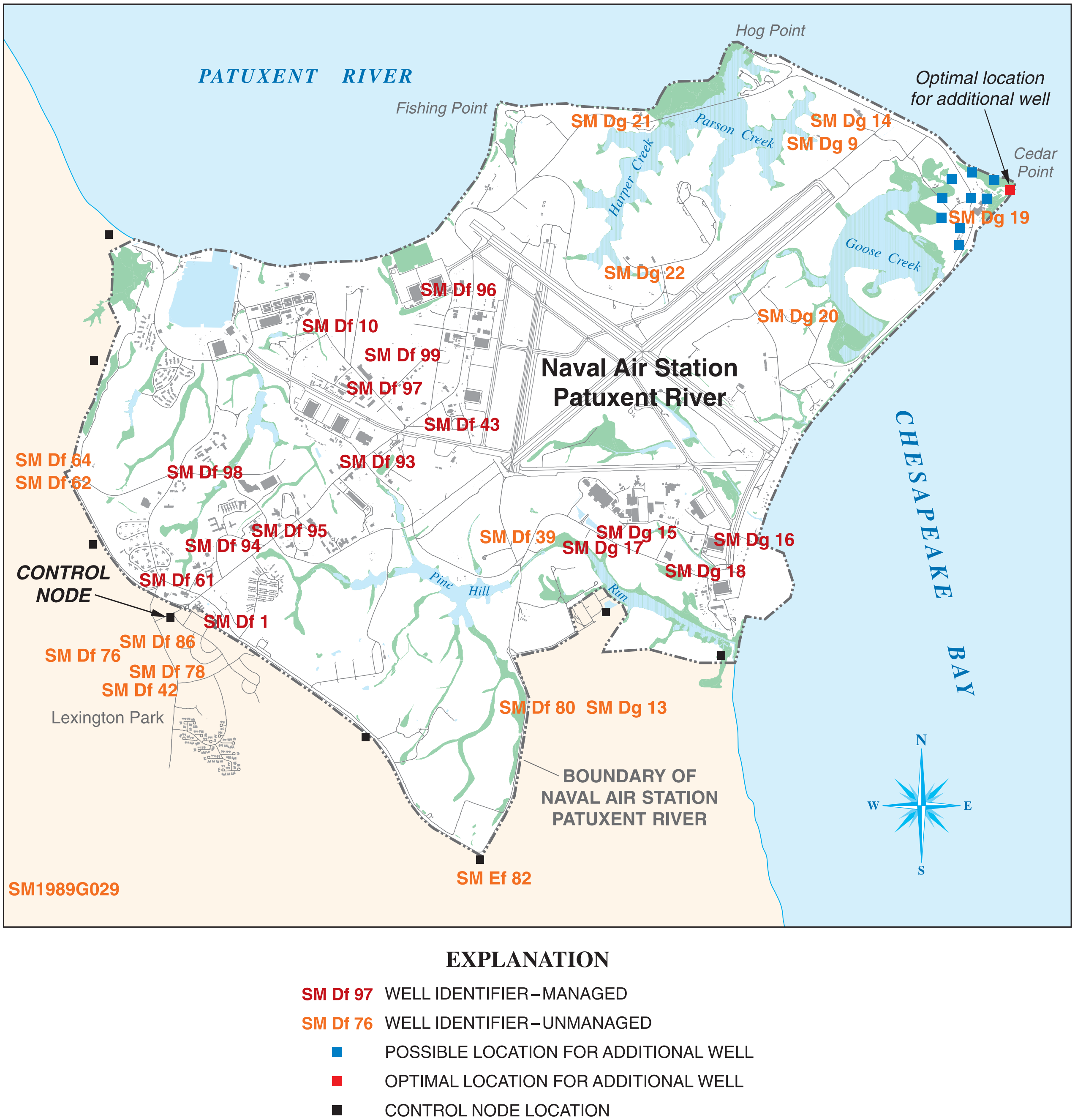

Figure 15. Location of ten potential well sites, including the optimal well site, for hypothetical optimization scenario 2 at Naval Air Station Patuxent River, Maryland.

Suggestions for Future Water-Supply Assessment

Water use continues to increase in southern Maryland and appropriations for new withdrawals have transitioned from the Aquia to the Upper Patapsco aquifer. For continued maximum benefit to the NAS Patuxent River, these changes would need to be incorporated into future ground-water-flow and optimization models. Since the modeling for this study was done, upgrades to the calibration process (Hill and others, 2000), and optimization modeling (Ahlfeld and others, 2005) have been made and could be incorporated into future modeling. Withdrawals from the Upper Patapsco aquifer at both the main air station and in surrounding communities have increased since 2002. The effects of these increased withdrawals could be assessed by use of the ground-water-flow and optimization models to properly manage the resource. Additionally, other non-hypothetical management scenarios with more complex constraints could be evaluated as wells at the main air station are installed or de-commissioned, or as withdrawal rates change. Additional constraints related to well efficiency, or saltwater intrusion, for example, could be applied. The models are also useful tools for understanding the regional ground-water-flow system in southern Maryland, and the effects of the NAS Patuxent River withdrawals on that flow system.

Summary and Conclusions

In southern Maryland, the Piney Point-Nanjemoy, Aquia, and Upper Patapsco aquifers are three of the six principal aquifers tapped for potable water in this area. These are also the three aquifers upon which the Naval Air Station (NAS) Patuxent River relies for their water supply. Water levels in these aquifers are below sea level (NAVD 88), and in the case of the Aquia aquifer, are as much as 170 feet below sea level, in the vicinity of Lexington Park, Maryland. The planners and engineers within the NAS Patuxent River Public Works Department are attempting to limit withdrawals by NAS Patuxent River so that they have minimal impact on the regional water levels within these three aquifers. To evaluate the effect of NAS Patuxent River withdrawals on the local flow system, the U.S. Geological Survey developed a ground-water-flow model. In order to minimize the effect of the NAS Patuxent River withdrawals on the local potentiometric surface of the Aquia aquifer, while still meeting the withdrawal needs of the main air station, the ground-water-flow model was coupled with an optimization model.

The ground-water-flow model for NAS Patuxent River includes the main air station and the immediate surroundings, including Lexington Park. The model is discretized into 102 rows by 118 columns. The intersection of adjacent rows and adjacent columns forms cells that are 250 by 250 feet on a side. The model in the vertical dimension is discretized into seven layers. Thus, there are a total of 84,252 cells, each with an area of about 1.4 acres. The model layering includes the three aquifers that are the source for the main air station water supply, the Piney Point-Nanjemoy, Aquia, and Upper Patapsco aquifers. A transient simulation representing 1900 through 2002 was calibrated to match simulated heads to observed heads over that period.

A steady-state ground-water-flow simulation was used to test the sensitivity of the model to various input parameters. The results of the model sensitivity analysis indicate that model-simulated heads are not sensitive to: increases or decreases in the horizontal hydraulic conductivity of the upper and middle confining units, decreases in the horizontal and vertical hydraulic conductivity of all confining units, decreases in withdrawal rates, increases or decreases in the horizontal hydraulic conductivity of layer 3, increases in general-head boundary conductance, or increases in the horizontal hydraulic conductivity of layer 5. In contrast, model-simulated heads are sensitive to: decreases in the horizontal hydraulic conductivity and large decreases (two orders of magnitude) in general-head boundary conductance. The model-simulated water levels also are sensitive to increases in withdrawal rates, and a two-orders-of-magnitude increase in the horizontal and vertical hydraulic conductivity of the confining units (layers 2, 4, and 6).

The steady-state ground-water-flow simulation was linked to the optimization model using MODMAN software. Two hypothetical optimization scenarios were evaluated. The first scenario was designed to determine the optimal pumping rates for wells screened in the Aquia aquifer within three supply groups (15 total wells) to meet a 25-percent increase in withdrawal demands, while minimizing the drawdown at a control location just outside the main air station boundary. The resulting optimal solution determined that pumping six wells above the rate required for maintenance produced the least amount of drawdown at the control location.

The second hypothetical scenario was designed to determine the optimal location for an additional well in the Aquia aquifer in the northeastern part of the main air station. The additional well was needed to meet an increase in withdrawal of 43,000 cubic feet per day. The optimization model was used to determine the optimal location for the new well, out of a possible 10 locations, while minimizing drawdown in the control nodes outside the western boundary of the main air station. The optimal location is about 1,500 feet to the east-northeast of the existing well.

Acknowledgments

The authors would like to thank the many personnel at Naval Air Station Patuxent River in the Public Works Department and the Environmental Support Group who assisted the project over the past 10 years. In addition, the authors thank the many reviewers of this report for their helpful comments, especially David Andreasen of the Maryland Geological Survey, and Charles Dunning of the U.S. Geological Survey Wisconsin Water Science Center.

Selected References

Achmad, Grufron, and Fewster, T.B., 2003, Delineation of zones of transport for public-supply wells in St. Mary's County, Maryland: Maryland Geological Survey Open-File Report No. 2003–02–16, 82 p.

Achmad, Grufron, and Hansen, H.J., 1997, Hydrogeology, model simulation, and water-supply potential of the Aquia and Piney Point-Nanjemoy aquifers in Calvert and St. Mary's Counties, Maryland: Maryland Geological Survey Report of Investigations No. 64, 197 p.

Achmad, Grufron, and Hansen, H.J., 2001a, Ground-water levels and pumpage trends in the major coastal plain aquifers of Southern Maryland between 1970 and 1996: Maryland Geological Survey Open-File Report No. 2001–02–12, 149 p.

Achmad, Grufron, and Hansen, H.J., 2001b, Simulated changes in water levels of the Aquia aquifer using revised water-use projections to 2025 for Calvert and St. Mary's Counties, Maryland: Maryland Geological Survey Supplemental Report No. S1/RI 64, 58 p.

Ahlfeld, D.P., Barlow, P.M., and Mulligan, A.E., 2005, GWM–A ground-water management process for the U.S. Geological Survey modular ground-water model (MODFLOW-2000): U.S. Geological Survey Open-File Report 2005–1072, 124 p.

Ahlfeld, D.P., and Mulligan, A.E., 2000, Optimal management of flow in groundwater systems: San Diego, California, Academic Press, 185 p.

Anderson, M.P., and Woessner, W.W., 1992, Applied groundwater modeling simulation of flow and advective transport: San Diego, California, Academic Press, 192 p.

Andreasen, D.C., 2007, Optimization of ground-water withdrawals in Anne Arundel County, Maryland, from the Upper Patapsco, Lower Patapsco, and Patuxent aquifers projected through 2044: Maryland Geological Survey Report of Investigations No. 77, 107 p.

Banks, W.S.L., and Dillow, J.A., 2001, Optimization of ground-water withdrawal at the Old O-Field area, Aberdeen Proving Ground, Maryland: U.S. Geological Survey Water-Resources Investigations Report 01–4083, 17 p.

Barlow, P.M., 2005, Use of simulation-optimization modeling to assess regional ground-water systems: U.S. Geological Survey Fact Sheet 2005–3095, 4 p.

Brown, P.M., Miller, J.A., and Swain, F.M., 1972, Structural and stratigraphic framework, and spatial distribution of permeability of the Atlantic Coastal Plain, North Carolina to New York: U.S. Geological Survey Professional Paper 796, 79 p.

Chapelle, F.H., and Drummond, D.D., 1983, Hydrogeology, digital simulation, and geochemistry of the Aquia and Piney Point-Nanjemoy aquifer system in Southern Maryland: Maryland Geological Survey Report of Investigations No. 38, 100 p.

Chapelle, F.H., Drummond, D.D., and Curley, Tracey, 1981, Map showing the potentiometric surface of the Aquia aquifer, May 19–23, 1980: U.S. Geological Survey Open-File Report 81–416, 1 p.

Chiang, W.-H., and Kinzelbach, Wolfgang, 1998, Processing modflow: a simulation system for modeling groundwater flow and pollution: Hamburg, Germany, Springer-Verlag, 325 p.

Clark, W.B., Mathews, E.G., and Berry, E.W., 1918, The surface and underground water resources of Maryland, including Delaware and the District of Columbia: Maryland Geological Survey, Special Publication, v. 10, pt. 2, 372 p.

Cooke, C.W., and Cloos, E., 1951, Geologic map of Prince Georges County, and the District of Columbia: Maryland Department of Geology, Mines, and Water Resources, scale 1:62,500.

Curtin, S.E., Andreasen, D.C., and Mack, F.K., 1993a, Potentiometric surface of the Aquia aquifer in Southern Maryland, September 1991: U.S. Geological Survey Open-File Report 93–652, 1 p.

Curtin, S.E., Andreasen, D.C., and Mack, F.K., 1993b, Potentiometric surface of the Upper Patapsco aquifer in Southern Maryland, September 1991: U.S. Geological Survey Open-File Report 93–654, 1 p.

Curtin, S.E., Andreasen, D.C., and Wheeler, J.C., 2001a, Potentiometric surface of the Aquia aquifer in Southern Maryland, September 1999: U.S. Geological Survey Open-File Report 01–204, 1 p.

Curtin, S.E., Andreasen, D.C., and Wheeler, J.C., 2001b, The difference between the potentiometric surfaces of the Aquia aquifer, September 1982 and September 1999 in Southern Maryland: U.S. Geological Survey Open-File Report 01–205, 1 p.

Curtin, S.E., Andreasen, D.C., and Wheeler, J.C., 2001c, Potentiometric surface of the Upper Patapsco aquifer in Southern Maryland, September 1999: U.S. Geological Survey Open-File Report 01–208, 1 p.

Curtin, S.E., Andreasen, D.C., and Wheeler, J.C., 2001d, The difference between the potentiometric surfaces of the Upper Patapsco aquifer, September 1982 and September 1999 in Southern Maryland: U.S. Geological Survey Open-File Report 01–209, 1 p.

Curtin, S.E., Andreasen, D.C., and Wheeler, J.C., 2002a, Potentiometric surface of the Aquia aquifer in Southern Maryland, September 2000: U.S. Geological Survey Open-File Report 02–244, 1 p.

Curtin, S.E., Andreasen, D.C., and Wheeler, J.C., 2002b, Potentiometric surface of the Upper Patapsco aquifer in Southern Maryland, September 2000: U.S. Geological Survey Open-File Report 02–246, 1 p.

Curtin, S.E., Andreasen, D.C., and Wheeler, J.C., 2002c, Potentiometric surface of the Aquia aquifer in Southern Maryland, September 2001: U.S. Geological Survey Open-File Report 02–442, 1 p.

Curtin, S.E., Andreasen, D.C., and Wheeler, J.C., 2002d, Potentiometric surface of the Upper Patapsco aquifer in Southern Maryland, September 2001: U.S. Geological Survey Open-File Report 02–446, 1 p.

Curtin, S.E., Andreasen, D.C., and Wheeler, J.C., 2002e, The difference between the potentiometric surfaces of the Aquia aquifer, September 1982 and September 2001 in Southern Maryland: U.S. Geological Survey Open-File Report 02–443, 1 p.

Curtin, S.E., Andreasen, D.C., and Wheeler, J.C., 2002f, The difference between the potentiometric surfaces of the Upper Patapsco aquifer, September 1982 and September 2001 in Southern Maryland: U.S. Geological Survey Open-File Report 02–447, 1 p.

Curtin, S.E., Andreasen, D.C., and Wheeler, J.C., 2003a, Potentiometric surface of the Aquia aquifer in Southern Maryland, September 2002: U.S. Geological Survey Open-File Report 03–255, 1 p.

Curtin, S.E., Andreasen, D.C., and Wheeler, J.C., 2003b, Potentiometric surface of the Upper Patapsco aquifer in Southern Maryland, September 2002: U.S. Geological Survey Open-File Report 03–257, 1 p.

Curtin, S.E., Andreasen, D.C., and Wheeler, J.C., 2005a, Potentiometric surface of the Aquia aquifer in Southern Maryland, September 2003: U.S. Geological Survey Open-File Report 2005–1004, 1 p.

Curtin, S.E., Andreasen, D.C., and Wheeler, J.C., 2005b, The difference between the potentiometric surfaces of the Aquia aquifer, September 1982 and September 2003 in Southern Maryland: U.S. Geological Survey Open-File Report 2005–1005, 1 p.

Curtin, S.E., Andreasen, D.C., and Wheeler, J.C., 2005c, Potentiometric surface of the Upper Patapsco aquifer in Southern Maryland, September 2003: U.S. Geological Survey Open-File Report 2005–1008, 1 p.

Curtin, S.E., Andreasen, D.C., and Wheeler, J.C., 2005d, The difference between the potentiometric surfaces of the Upper Patapsco aquifer, September 1990 and September 2003 in Southern Maryland: U.S. Geological Survey Open-File Report 2005–1009, 1 p.

Curtin, S.E., and Dine, J.R., 1995, Ground-water level data in Southern Maryland, 1946–94: Maryland Geological Survey Basic Data Report No. 21, 365 p.

Curtin, S.E., Mack, F.K., and Andreasen, D.C., 1994a, Potentiometric surface of the Aquia aquifer in Southern Maryland, September 1993: U.S. Geological Survey Open-File Report 94–390, 1 p.

Curtin, S.E., Mack, F.K., and Andreasen, D.C., 1994b, The difference between the potentiometric surfaces of the Aquia aquifer, September 1982 and September 1993 in Southern Maryland: U.S. Geological Survey Open-File Report 94–394, 1 p.

Curtin, S.E., Mack, F.K., and Andreasen, D.C., 1994c, Potentiometric surface of the Upper Patapsco aquifer in Southern Maryland, September 1993: U.S. Geological Survey Open-File Report 94–392, 1 p.

Curtin, S.E., Mack, F.K., and Andreasen, D.C., 1995a, Potentiometric surface of the Aquia aquifer in Southern Maryland, September 1994: U.S. Geological Survey Open-File Report 95–743, 1 p.

Curtin, S.E., Mack, F.K., and Andreasen, D.C., 1995b, Potentiometric surface of the Upper Patapsco aquifer in Southern Maryland, September 1994: U.S. Geological Survey Open-File Report 95–745, 1 p.

Curtin, S.E., Mack, F.K., and Andreasen, D.C., 1996a, Potentiometric surface of the Aquia aquifer in Southern Maryland, September 1995: U.S. Geological Survey Open-File Report 96–620, 1 p.

Curtin, S.E., Mack, F.K., and Andreasen, D.C., 1996b, The difference between the potentiometric surfaces of the Aquia aquifer, September 1982 and September 1995 in Southern Maryland: U.S. Geological Survey Open-File Report 96–624, 1 p.

Curtin, S.E., Mack, F.K., and Andreasen, D.C., 1996c, Potentiometric surface of the Upper Patapsco aquifer in Southern Maryland, September 1995: U.S. Geological Survey Open-File Report 96–622, 1 p.

Curtin, S.E., Mack, F.K., and Andreasen, D.C., 1997a, Potentiometric surface of the Aquia aquifer in Southern Maryland, September–October 1996: U.S. Geological Survey Open-File Report 97–788, 1 p.

Curtin, S.E., Mack, F.K., and Andreasen, D.C., 1997b, Potentiometric surface of the Upper Patapsco aquifer in Southern Maryland, September-October 1996: U.S. Geological Survey Open-File Report 97–790, 1 p.

Curtin, S.E., Mack, F.K., and Andreasen, D.C., 1999a, Potentiometric surface of the Aquia aquifer in Southern Maryland, September 1997: U.S. Geological Survey Open-File Report 99–82, 1 p.

Curtin, S.E., Mack, F.K., and Andreasen, D.C., 1999b, Potentiometric surface of the Upper Patapsco aquifer in Southern Maryland, September 1997: U.S. Geological Survey Open-File Report 99–85, 1 p.

Curtin, S.E., Mack, F.K., and Andreasen, D.C., 1999c, The difference between the potentiometric surfaces of the Aquia aquifer, September 1982 and September 1997 in Southern Maryland: U.S. Geological Survey Open-File Report 99–81, 1 p.

Curtin, S.E., Mack, F.K., and Andreasen, D.C., 1999d, The difference between the potentiometric surfaces of the Upper Patapsco aquifer, September 1990 and September 1997 in Southern Maryland: U.S. Geological Survey Open-File Report 99–86, 1 p.

Curtin, S.E., Mack, F.K., and Andreasen, D.C., 2000a, Potentiometric surface of the Aquia aquifer in Southern Maryland, September 1998: U.S. Geological Survey Open-File Report 00–83, 1 p.

Curtin, S.E., Mack, F.K., and Andreasen, D.C., 2000b, Potentiometric surface of the Upper Patapsco aquifer in Southern Maryland, September 1998: U.S. Geological Survey Open-File Report 00–85, 1 p.

Czarnecki, J.B., Clark, B.R., and Stanton, G.P., 2003, Conjunctive-use optimization model of the Mississippi River Valley alluvial aquifer of southeastern Arkansas: U.S. Geological Survey Water-Resources Investigations Report 03–4233, 26 p.

Deninger, R.A., 1970, Systems analysis of water supply systems: Water Resources Bulletin, v. 6, no. 4, p. 573–579.

Domenico, P.A., and Schwartz, F.W., 1990, Physical and chemical hydrogeology: New York, John Wiley & Sons, 824 p.

Drummond, D.D., 1984, Records of selected wells, Calvert and St. Mary's Counties, Maryland: Maryland Geological Survey Water Resources Basic Data Report No. 14, 117 p.

Drummond, D.D., 2005, Water-supply potential of the Coastal Plain aquifers in Calvert, Charles, and St. Mary's Counties, Maryland, with emphasis on the Upper Patapsco and Lower Patapsco aquifers: Maryland Geological Survey Administrative Report, June 2005, accessed July 23, 2007, at *http://www.mgs.md.gov/hydro/pub/pdf/smdadmin.pdf*

Ferguson, H.F., 1953, The ground water resources in The water resources of St Mary's County: Maryland Department of Geology, Mines and Water Resources, Bulletin 11, 180 p.

Fetter, C.W., 1994, Applied hydrogeology (3d ed.): New York, Macmillan College Publishing Co., 691 p.

Fleck, W.B., 1983, Metropolitan Washington, D.C. area water supply study, Maryland, Virginia, and the District of Columbia: U.S. Army Corps of Engineers, Baltimore, Maryland, Appendix F, p. 131–184.

Fleck, W.B., and Vroblesky, D.A., 1996, Simulation of ground-water flow of the Coastal Plain aquifers in parts of Maryland, Delaware, and the District of Columbia: U.S. Geological Survey Professional Paper 1404–J, 41 p., 9 pls.

Forstall, R.L., 1995, Maryland population of counties by decennial census: 1900 to 1990: U.S. Bureau of the Census, accessed January 12, 2004, at *http://www.census.gov/population/cencounts/md190090.txt*

Freeze, R.A., and Cherry, J.A., 1979, Groundwater: Englewood Cliffs, New Jersey, Prentice-Hall, Inc., 604 p.

Glaser, J.D., 1976, Geologic map of Anne Arundel County: Maryland Geological Survey, scale 1:62,500.

Gorelick, S.M., 1983, A review of distributed parameter groundwater management modeling methods: Water Resources Research, v. 19, no. 2, p. 305–319.

Granato, G.E., and Barlow, P.M., 2005, Effects of alternative instream-flow criteria and water-supply demands on ground-water development options in the Big River area, Rhode Island: U.S. Geological Survey Scientific Investigations Report 2004–5301, 110 p.

Greenwald, R.M., 1998a, Documentation and user's guide—MODMAN, an optimization module for MODFLOW, version 4.0: Freehold, New Jersey, HIS GeoTrans, Inc., [variously paged].

Greenwald, R.M., 1998b, MODMAN 4.0 windows-based preprocessor-version 1.02: Freehold, New Jersey, HIS GeoTrans, Inc., [variously paged].

Hack, J.T., 1977, Geologic map for land-use planning, Prince Georges County, Maryland: U.S. Geological Survey Miscellaneous Investigation Series Map I–1004, scale 1:62,500.

Hansen, H.J., 1972, A user's guide for the artesian aquifers of the Maryland Coastal Plain, part two: Aquifer characteristics: Maryland Geological Survey, 123 p.

Hansen, H.J., 1974, Sedimentary facies of the Aquia Formation in the subsurface of the Maryland Coastal Plain: Maryland Geological Survey Report of Investigations No. 21, 47 p.

Hansen, H.J., 1977, Geologic and hydrologic data from two core holes drilled through the Aquia Formation (Eocene-Paleocene) in Prince George's and Queen Anne's Counties, Maryland: Maryland Geological Survey Miscellaneous Open-File Report, 77 p.

Hansen, H J., and Wilson, J.M., 1984, Summary of hydrogeologic data from a deep (2,678 ft.) well at Lexington Park, St. Mary's County, Maryland: Maryland Geological Survey Open-File Report No. 84–02–1, 61 p.

Harbaugh, A.W., and McDonald, M.G., 1996, User's documentation for MODFLOW-96, an update to the U.S. Geological Survey modular finite-difference ground-water flow model: U.S. Geological Survey Open-File Report 96–485, 56 p.

Hill, M.C., Banta, E.R., Harbaugh, A.W., and Anderman, E.R., 2000, MODFLOW-2000, the U.S. Geological Survey modular ground-water model – User guide to the observation, sensitivity, and parameter-estimation processes and three post-processing programs: U.S. Geological Survey Open-File Report 00-184, 209 p.

HyperLINDO/PC, 1998, Computer software (Release 6.01): Chicago, Illinois, LINDO Systems, Inc.

Kapple, G.W., and Hansen, H.J., 1976, A digital simulation model of the Aquia aquifer in Southern Maryland: Maryland Geological Survey Circular 20, 33 p.

Klohe, C.A., and Feehley, C.E., 2001, Hydrogeology and ground-water quality of the Piney Point-Nanjemoy and Aquia aquifers, Naval Air Station Patuxent River and Webster Outlying Field, St. Mary's County, Maryland: U.S. Geological Survey Water-Resources Investigations Report 01–4029, 51 p.

Klohe, C.A., and Kay, R.T., 2007, Hydrogeology of the Piney Point-Nanjemoy, Aquia, and Upper Patapsco aquifers, Naval Air Station Patuxent River and Webster Outlying Field, St. Marys County, Maryland, 2000-06: U.S. Geological Survey Scientific Investigations Report 2006–5266, 26 p.

Lee, K., and Fetter, C.W., 1994, Hydrogeology laboratory manual: New York, Macmillan Publishing Co., 135 p.

Lindo Systems Inc., 2001, LINDO User's manual: Chicago, Illinois, 296 p.

Mack, F.K., 1974, An evaluation of the Magothy aquifer in the Annapolis area, Maryland: Maryland Geological Survey Report of Investigations No. 22, 75 p.

Mack, F.K., Andreasen, D.C., Curtin, S.E., and Wheeler, J.C., 1987a, Potentiometric surface of the Aquia aquifer in Southern Maryland during the fall of 1986: U.S. Geological Survey Water-Resources Investigations Report 87–4214, 1 p.

Mack, F.K., Andreasen, D.C., Curtin, S.E., and Wheeler, J.C., 1987b, Difference between the potentiometric surfaces of the Aquia aquifer in the spring of 1979 and fall of 1986 in Southern Maryland: U.S. Geological Survey Water-Resources Investigations Report 87–4215, 1 p.

Mack, F.K., Andreasen, D.C., Curtin, S.E., and Wheeler, J.C., 1989, Potentiometric surface of the Aquia aquifer in Southern Maryland during the fall of 1987: U.S. Geological Survey Water-Resources Investigations Report 89-4012, 1 p.

Mack, F.K., Andreasen, D.C., Curtin, S.E., and Wheeler, J.C., 1990a, Potentiometric surface of the Aquia aquifer in Southern Maryland during the fall of 1988: U.S. Geological Survey Water-Resources Investigations Report 87–4037, 1 p.

Mack, F.K., Andreasen, D.C., Curtin, S.E., and Wheeler, J.C., 1990b, The difference between the potentiometric surfaces of the Aquia aquifer of September 1986 and September 1988 in Southern Maryland: U.S. Geological Survey Water-Resources Investigations Report 90–4039, 1 p.

Mack, F.K., Curtin, S.E., Andreasen, D.C., and Wheeler, J.C., 1991, Potentiometric surface of the Aquia aquifer in Southern Maryland, September 1989: U.S. Geological Survey Open-File Report 91–4094, 1 p.

Mack, F.K., Curtin, S.E., Andreasen, D.C., and Wheeler, J.C., 1992a, The difference between the potentiometric surfaces of the Aquia aquifer of September 1982 and September 1990 in Southern Maryland: U.S. Geological Survey Open-File Report 92–463, 1 p.

Mack, F.K., Curtin, S.E., Andreasen, D.C., and Wheeler, J.C., 1992b, Potentiometric surface of the Aquia aquifer in Southern Maryland, September 1990: U.S. Geological Survey Open-File Report 92–459, 1 p.

Mack, F.K., Curtin, S.E., Andreasen, D.C., and Wheeler, J.C., 1992c, Potentiometric surface of the Upper Patapsco aquifer in Southern Maryland, September 1990: U.S. Geological Survey Open-File Report 92–461, 1 p.

Mack, F.K., Wheeler, J.C., and Curtin, S.E., 1983a, Preliminary map showing the potentiometric surface of the Aquia aquifer in Southern Maryland, September 1982: U.S. Geological Survey Open-File Report 83–929, 1 p.

Mack, F.K., Wheeler, J.C., and Curtin, S.E., 1983b, Preliminary map showing the difference between the potentiometric surfaces of the Aquia aquifer of April 1979 and September 1982 in Southern Maryland: U.S. Geological Survey Open-File Report 83–930, 1 p.

Mack, F.K., Wheeler, J.C., Curtin, S.E., and Andreasen, D.C., 1985a, Preliminary map showing the potentiometric surface of the Aquia aquifer in Southern Maryland, September 1984: U.S. Geological Survey Open-File Report 85–4338, 1 p.

Mack, F.K., Wheeler, J.C., Curtin, S.E., and Andreasen, D.C., 1985b, Preliminary map showing the difference between the potentiometric surfaces of the Aquia aquifer of September 1982 and September 1984 in Southern Maryland: U.S. Geological Survey Open-File Report 85–4339, 1 p.

Mack, F.K., Wheeler, J.C., Curtin, S.E., and Andreasen, D.C., 1987, Potentiometric surface of the Aquia aquifer in Southern Maryland, September 1985: U.S. Geological Survey Water-Resources Investigations Report 87–4029, 1 p.

Maryland Department of Planning, 2007, Maryland State Data Center population projections, revised October 2007, [variously paged]: accessed June 10, 2008, at *http://www.mdp.state.md.us/msdc/popproj/TOTPOP_PROJ07.pdf*

Mathews, E.B., 1933, Map of Maryland showing geologic formations: Maryland Geological Survey, scale 1:380,160.

McCartan, Lucy, 1989, Geologic map of St. Mary's County: Maryland Geological Survey, scale 1:62,500.

McDonald, M.G., and Harbaugh, A.W., 1984, A modular three-dimensional finite-difference ground-water flow model: U.S. Geological Survey Open-File Report 83–875, 528 p.

Otton, E.G., 1955, Ground-water resources of the Southern Maryland Coastal Plain: Maryland Department of Geology, Mines and Water Resources, Bulletin 15, 347 p.

Overbeck, R.M., 1951, Ground-water resources in The water resources of Calvert County: Maryland Department of Geology, Mines and Water Resources, Bulletin 8, 97 p.

Pollock, D.W., 1994, User's guide for MODPATH/ MODPATH-PLOT, version 3: a particle-tracking post-processing package for MODFLOW, the U.S. Geological Survey finite-difference ground-water flow model: U.S. Geological Survey Open-File Report 94–464, [variously paged].

Reilly, T.E., and Harbaugh, A.W., 2004, Guidelines for evaluating ground-water-flow models: U.S. Geological Survey Scientific Investigations Report 2004–5038, 30 p.

Schrage, L.E., 1997, Optimization modeling with LINDO: Pacific Grove, California, Duxbury Press, 470 p.

U.S. Census Bureau, 2003, State and county quick facts, Maryland, [variously paged]: accessed January 12, 2004, at *http://quickfacts.census.gov/qfd/states/24000.html*

United States Navy, 2003, NAS Patuxent River, [variously paged]: accessed May 15, 2003, at *http://nas.nawcad.navy.mil/*

Vroblesky, D.A., and Fleck, W.B., 1991, Hydrogeologic framework of the Coastal Plain of Maryland, Delaware, and the District of Columbia, regional aquifer-system analysis—northern Atlantic Coastal Plain: U.S. Geological Survey Professional Paper 1404–E, 45 p.

Wagner, B.J., 1995, Recent advances in simulation-optimization groundwater management modeling: U.S. National Report to IUGG, 1991–1994, Rev Geophysics. v. 33 suppl., American Geophysical Union, p. 1021–1028.

Walton, W.C., 1970, Groundwater resource evaluation: New York, McGraw-Hill Book Co., 664 p.

Weigle, J.M., and Webb, W.E., 1970, Southern Maryland records of selected wells, water levels and chemical analyses of water: Maryland Geological Survey Basic Data Report No. 4, 48 p.

Williams, J.F., III, 1979, Simulated changes in water level in the Piney Point aquifer in Maryland: Maryland Geological Survey Report of Investigations No. 31, 49 p.

Glossary

aquifer A saturated unit that is part of one or more formations and yields water in sufficient quantity to be a viable source of potable water (Walton, 1970, p. 29).

conductance (on general-head boundary) A combination of several parameters in Darcy's law so that Darcy's law can be expressed as:

$$Q = C(h_2 - h_1)$$

where
- Q is the flow ($L^3 T^{-1}$);
- $h_1 - h_2$ is the head difference across the length of the boundary (L); and
- C is conductance ($L^2 T^{-1}$) and is defined as:

$$C = KA / L$$

where
- K is the hydraulic conductivity of the material in the direction of flow ($L\,T^{-1}$);
- A is the cross-sectional area perpendicular to flow (L^2); and
- L is the length of the flow path (L) (McDonald and Harbaugh, 1984, p. 130).

confining unit Arbitrarily defined as a geologic layer in which the hydraulic conductivity is less than about 3 x 10^{-2} ft/d (Fetter, 1994, p. 110). Generally, ground water moves through confining layers very slowly.

hydraulic conductivity The volume of water that moves in a unit of time through a unit cross section under a unit hydraulic gradient ($L^3 T^{-1}/L^2$).

porosity The part of the rock or sediment that is void space and is expressed as a percentage of the total volume (Domenico and Schwartz, 1990).

specific capacity The productivity of a well, given as the pumping rate of the well per unit of drawdown (from Freeze and Cherry, 1979, p. 313–314).

specific yield Aquifer tests are not normally performed on new wells. Newly installed wells are typically pumped at a set rate for a few hours and the maximum drawdown is recorded, however. The pumping rate divided by the drawdown is the specific yield (Fetter, 1994, p. 256).

transmissivity The volume of water that passes through a vertical section of unit width through the full thickness of the aquifer under a unit head (egg unit hydraulic gradient of 45 degrees) per day and is expressed in units of cubic feet per foot of thickness per day ($L^3 T^{-1} L\pm$), or in its reduced form as feet squared per day (ft^2/d).

Appendix 1. Specific Capacity Analysis

Hydraulic conductivities for the three principal aquifers that are used in the area of NAS Patuxent River were determined from specific capacity analysis. Theis (1963) developed an equation to calculate transmissivity from specific capacity:

$$T = \frac{2.3Y}{4\pi} \log\left(\frac{2.25Tt}{r^2 S}\right) \qquad (1)$$

where
- T is transmissivity ($L^2 T^{-1}$);
- Y is specific capacity for fully penetrating well ($L^2 T^{-1}$);
- t is time (T);
- r is pumping well radius (L); and
- S is aquifer storativity (dimensionless).

This equation assumes that the well is screened across the full thickness of the aquifer. To account for wells screened across only a part of the aquifer, a correction was made using the Kozeny equation (Johnson, 1966, p. 134; Kozeny, 1933, p. 104):

$$Y = \frac{Y_p}{p\left(1 + 7\left(\frac{r}{2bp}\right)^{0.5}\right)\cos\frac{\pi b}{2}} \qquad (2)$$

where
- Y_p is specific capacity for a well partially screened across full thickness ($L^2 T^{-1}$);
- b is aquifer thickness (L); and
- p is the ratio of the screen to the aquifer thickness (dimensionless).

There were 186, 83, and 7 specific capacity analyses for the Piney Point-Nanjemoy, Aquia, and Upper Patapsco aquifers, respectively, for an area extending about 10 miles outward from the NAS Patuxent River. The median, first quartile, and third quartile values of the calculated hydraulic conductivity values are shown in table A1.

Within the confines of the model area, there were 11 specific capacity analyses for the Piney Point-Nanjemoy aquifer. From these 11 analyses, hydraulic conductivity values were calculated using equations 1 and 2. The median hydraulic conductivity value for the Piney Point-Nanjemoy aquifer in the model area is 15 feet per day as indicated in table A1. Similarly, the median value for the Aquia aquifer in the model area is 20 feet per day. There is only one value for the Upper Patapsco aquifer in the model area, 45 feet per day.

References

Johnson, E.E., Inc., 1966, Ground water and wells (1st ed.): Saint Paul, Minnesota, Edward E. Johnson, Inc., 440 p.

Kozeny, Josef, 1933, Theorie und berechnung der brunnen: Wasserkraft und Wasserwirtschaft, v. 28, no. 9, p. 101–105.

Theis, C.V., 1963, Estimating the transmissivity of a water-table aquifer from the specific capacity of a well: U.S. Geological Survey Water Supply Paper 1536–I, p. 332–336.

Table A1. Statistical estimates of horizontal hydraulic conductivity calculated from specific capacity values.

	Horizontal hydraulic conductivity (feet per day)			
Aquifer and area	**Number of values**	**Median**	**First quartile**	**Third quartile**
Piney Point-Nanjemoy Aquifer				
Local area	186	20	12	42
Model area	11	15	10	17
Aquia Aquifer				
Local area	83	28	20	50
Model area	30	20	20	50
Upper Patapsco Aquifer				
Local area	7	24	18	39
Model area	1	45	Not calculated	Not calculated

Prepared by West Trenton, NJ Publishing Service Center.
Edited by Valerie M. Gaine.
Graphics by Timothy W. Auer.
Layout by Denis K. Sun.

For additional information, contact:
Director, MD-DE-DC Water Science Center
U.S. Geological Survey
5522 Research Park Drive
Baltimore, MD 21228

or visit our Web site at:
http://md.water.usgs.gov

Dieter, C.A. and Fleck, W.B.—**Simulation of Ground-Water Flow and Optimization of Withdrawals from Aquifers Underlying the Naval Air Station Patuxent River, St. Mary's County, Maryland**—USGS Scientific Investigations Report 2008–5144